1962

Experimental measurement of the mechanical impedance of a cantilever beam.

Hoover, Richard M.

Monterey, California: U.S. Naval Postgraduate School

EXPERIMENTAL MEASUREMENT OF THE MECHANICAL IMPEDANCE OF A CANTILEVER BEAM

RICHARD M. HOOVER

EXPERIMENTAL MEASUREMENT OF THE MECHANICAL IMPEDANCE OF A CANTILEVER BEAM

by

Richard M. Hoover
Lieutenant Commander, United States Navy

Submitted in partial fulfillment of
the requirements for the degree of

MASTER OF SCIENCE

IN

MECHANICAL ENGINEERING

United States Naval Postgraduate School
Monterey, California

1962

EXPERIMENTAL MEASUREMENT OF THE MECHANICAL IMPEDANCE OF A CANTILEVER BEAM

by

Richard M. Hoover

This work is accepted as fulfilling
the thesis requirements for the degree of
MASTER OF SCIENCE
IN
MECHANICAL ENGINEERING
from the
United States Naval Postgraduate School

ABSTRACT

In order to gain facility with mechanical impedance methods, and to determine the feasibility of using theoretical impedance functions in the design of machinery foundations, the mechanical impedance of a tip-driven cantilever beam of uniform cross section was determined experimentally. This experimental impedance function is compared with a theoretical impedance function. Correlation between the two impedance functions is good at the first resonant and the first antiresonant frequencies. Attachment of the means of driving the cantilever beam and measuring its resulting motion appears to modify the nature of the structure and its response to an exciting force. The accuracy of the experimental impedance function is limited by the accuracy of the phase angle determinations. A clamping jig for achieving experimentally the clamped end condition is described. The validity of the assumptions of linearity and negligible damping is established qualitatively. A method of checking theoretical relations, experimental procedures and proper functioning of instruments is also described.

The author wishes to express his appreciation for the assistance and encouragement given him in this investigation by Professor Ernest K. Gatcombe, Professor William C. Smith, Mr. Kenneth Mothersell and Mr. Robert Smith of the U. S. Naval Postgraduate School.

TABLE OF CONTENTS

TABLE OF CONTENTS

LIST OF ILLUSTRATIONS

LIST OF ILLUSTRATIONS

LIST OF SYMBOLS

Symbol	Name	Units
A	area of cross section	in^2
a	acceleration	in/sec^2
a_0	acceleration magnitude	in/sec^2
b	width of beam	in
C	electrical capacitance	farads or pf
E	Young's modulus	lbf/in^2
	transducer sensitivity	rms mv/peak g rms mv/peak lbf
e	base of natural logarithms (2.71828...)	
F	force	lbf
F_0	force magnitude	lbf
f	frequency of excitation	cps
G	Cathode follower gain	
g	acceleration due to gravity ($g = 386$ in/sec^2)	
h	depth of beam	in
I	moment of inertia	in^4
i	loop current (Appendix C)	amp
j	imaginary unit ($j = \sqrt{-1}$)	
ℓ	free length of cantilever beam	in
M	effective mass	lbm
M_0	effective mass magnitude	lbm
m	mass	lbm

TABLE OF SYMBOLS

Symbols	Name	Units
R	electrical resistance	ohms
t	time	sec
V_a	sinusoidal voltage proportional to acceleration	mv rms
V_F	sinusoidal voltage proportional to force	mv rms
V_1, V_2	reference voltages	
v	velocity	in/sec
v_0	velocity magnitude	in/sec
X_C	capacitive reactance ($X_C = \frac{1}{\omega C}$)	ohms
x	displacement in equation (8)	in
	distance from the clamped end of the beam in equation (14)	in
x_0	displacement magnitude	in
Z	mechanical impedance	lbf-sec/in
Z_0	mechanical impedance magnitude	lbf-sec/in
α	a phase angle. See equation (3-C)	deg
	receptance function. See equation (14)	in/lbf
θ	phase angle by which force leads acceleration in simple harmonic motion	deg
λ	$\lambda^4 = \frac{\omega^2 A \rho}{EI}$ See equations (14) and (15)	in^{-1}

TABLE OF SYMBOLS

Symbols	Name	Units
π	π = 3.1416...	
ρ	mass density	lbm/in^3
ϕ	phase angle by which force leads velocity in simple harmonic motion	deg
ω	circular frequency ($\omega = 2\pi f$)	rad/sec

1. Introduction

1.1 General

This study was undertaken in order to gain facility in the use of mechanical impedance methods for the analysis of forced vibrations of mechanical structures. A second objective was to determine, if possible, the feasibility of using theoretical impedance functions to check the design of structures such as machinery foundations. Such a check could be used to avoid designing foundations which have resonant frequencies at or near the exciting frequencies of the supported machine. It was proposed to determine the mechanical impedance of a cantilever beam experimentally, and compare the resulting impedance function with the mechanical impedance derived theoretically.

1.2 Mechanical Impedance

Mechanical impedance is a measure of the resistance of a structure to motion. Using mechanical impedance methods it is possible to describe the response of complicated structures to exciting forces. The use of the classical method of differential equations to describe the response of such structures, (the hull of a submarine, for example,) would be difficult or impossible.

Mechanical impedance is not a new concept, nor is it an old one. It is 'old' in the sense that many mechanical engineers know something about it. At the same time, however, the evolution of the concept has been such that the terminology for describing mechanical impedance has been standardized only recently. [1, 2]

The mechanical impedance concept will not be developed in this thesis since it has been developed in considerable detail in a number of references, some of which are listed in the bibliography. [2-10]

References 3, 4, 5 and 6 are particularly recommended to those to whom mechanical impedance is a new or unfamiliar concept.

Mechanical impedance Z is defined as the complex ratio of force to velocity. [1, 5]

$$Z = \frac{F}{v} \tag{1}$$

In the general case, both force F and velocity v are complex functions of the exciting frequency f. Thus, if we use the complex notation

$$F = F_0 e^{j(\omega t + \phi)} \tag{2}$$

$$v = v_0 e^{j\omega t} \tag{3}$$

equation (1) may be written

$$Z = \frac{F}{v} = \frac{F_0 e^{j(\omega t + \phi)}}{v_0 e^{j\omega t}} = \frac{F_0 e^{j\phi}}{v_0} = Z_0 e^{j\phi} \tag{4}$$

where F_0 is the magnitude of the exciting force,

v_0 is the magnitude of the resulting velocity,

$\omega = 2\pi f$ is the circular frequency of the exciting force,

ϕ is the phase angle between force and velocity,

Z_0 is the magnitude of the mechanical impedance, and

F_0, v_0, Z_0, and ϕ are all functions of the exciting frequency f.

If it is assumed that the structure is linear and elastic, and that it is excited by a sinusoidally varying force of frequency f, the resulting motion of any point in the structure will be directly proportional to the exciting force and at the same frequency. [5]

In this study, the cantilever beam was excited sinusoidally and damping in the system was assumed to be negligible. With these simplifications, equations (2), (3) and (4) become

$$F = F_0 \cos(\omega t + \phi) \tag{5}$$

$$v = v_0 \cos \omega t \tag{6}$$

$$Z = \frac{F}{v} = \frac{F_0 \cos(\omega t + \phi)}{v_0 \cos \omega t} = Z_0 \angle \phi \tag{7}$$

where F_0, v_0, Z_0 and ϕ are functions of the exciting frequency f.

Thus mechanical impedance is a frequency-dependent function which relates the force exciting a structure to the resultant motion of some point in the structure. If

the force and velocity are measured at the same point, the ratio of these two quantities is called a driving-point impedance. If they are measured at different points, the ratio is designated a transfer impedance. Both driving-point and transfer impedances were determined in this study.

It may be seen from equation (7) that the experimental determination of mechanical impedance involves the measurement of F_0, v_0, and ϕ at each value of frequency f.

1.3 Effective Mass

One advantage to exciting a structure sinusoidally is that displacement or acceleration may be observed instead of velocity. Displacement or acceleration amplitudes may then be converted to velocity amplitude by multiplying or dividing by ω as necessary in accordance with the following familiar relationships:

$$x = x_0 \cos \omega t \tag{8}$$

$$v = \dot{x} = -\omega x_0 \sin \omega t = v_0 \sin \omega t \tag{9}$$

$$a = \ddot{x} = -\omega^2 x_0 \cos \omega t = a_0 \cos \omega t \tag{10}$$

In this study, acceleration was observed in lieu of velocity. The ratio of sinusoidal exciting force to the resultant sinusoidal acceleration of a point in a structure is defined as effective mass, M. [2] This same ratio has

also been referred to as 'apparent mass' and 'apparent weight.' [5, 11]

Thus

$$M = \frac{F}{a} = \frac{F_0 \cos(\omega t + \theta)}{a_0 \cos \omega t} = M_0 \angle \theta \qquad (11)$$

where M_0, F_0, a_0, and θ are all functions of the exciting frequency f. In this study, M, F and a are not complex since linearity and negligible damping have been assumed. θ is the phase angle between force and acceleration. It is the angle by which the sinusoidal exciting force leads the resultant sinusoidal acceleration.

It may be seen that

$$Z_0 = \frac{F_0}{v_0} = \frac{\omega F_0}{a_0} = \omega M_0 \qquad (12)$$

and that

$$\phi = \theta + \frac{\pi}{2} \qquad (13)$$

1.4 Receptance Functions

Prior to the recent standardization of terminology, [1, 2] a number of investigators (chiefly in Great Britain) used the ratio of force to displacement and the reciprocal of this ratio to describe the response of various structures to vibratory forces. [12-15] The ratio of force to displacement in a linear system has been

called a 'dynamic flexibility'; while the ratio of displacement to force has been described as an 'admittance' or 'receptance' function.

In references 14 and 15 a number of receptance functions for beams in flexure are derived. In these derivations linearity and negligible damping have been assumed. These receptances are functions of the physical dimensions and properties of the beam and the frequency of the exciting force. They are developed from the differential equations of motion for the beams. The receptance function for a tip-driven cantilever, which is derived in reference 14, was used as the theoretical basis for this investigation. Equation (14) is a mathematical formulation of this receptance function.

$$\alpha_{x\ell} = \frac{F_7(\cos \lambda x - \cosh \lambda x) - F_9(\sin \lambda x - \sinh \lambda x)}{-2\ EI\ \lambda^3 F_4} \qquad (14)$$

$\alpha_{x\ell}$ is a receptance function which is the ratio of the displacement at x to a harmonically varying force applied at ℓ.

x is the distance from the clamped end of the beam

ℓ is the free length of the beam

E is Young's modulus

I is the moment of inertia of the cross section about the flexural axis

$$\lambda^4 = \frac{\omega^2 A \rho}{EI} \qquad (15)$$

ω is the angular frequency of the exciting force

ρ is the mass density

$$F_4 = \cos \ell \cosh \ell + 1 \tag{16}$$

$$F_7 = \sin \ell + \sinh \ell \tag{17}$$

$$F_9 = \cos \ell + \cosh \ell \tag{18}$$

1.5 Plotting Impedance Functions

A convenient manner of presenting impedance, receptance and effective mass functions is to plot them as ordinates against frequency as abscissae, usually on logarithmic graph paper. Since the magnitudes of dynamic stiffness $\frac{F_0}{x_0}$ and effective mass $\frac{F_0}{a_0}$ differ from the magnitude of mechanical impedance $\frac{F_0}{v_0}$ only by the factor ω, it is possible to construct graph paper on which any of these three functions may be plotted as a function of frequency. The value of the other two functions may then be read directly on appropriate scales. Such graph paper is available commercially. The impedance curves in this thesis were originally plotted as M vs f curves and then replotted for reproduction herein as Z vs f curves.

1.6 Problems Involved in Obtaining Mathematical End Conditions

Among the more challenging problems encountered in the experimental phase of this investigation were those concerned with (a) approximating the 'clamped' end condition, and (b) driving the beam in a direction perpendicular to its equilibrium position without loading the beam significantly. The manner in which these problems were solved is considered in Sections 2.3 and 2.4.

2. Description of Experimental Equipment

2.1 Preliminary Investigation

In order to gain familiarity with the instrumentation and to determine the validity of a number of theoretical relationships, the effective mass of a cylindrical brass mass was determined. The results of this preliminary investigation may be found in Section 3.1.

The arrangement for supporting and driving the brass mass is illustrated in Fig. 1. The force generator used in driving the brass mass (and subsequently in driving the cantilever beam) was a Goodmans Type 390A (permanent magnet) Vibration Generator.

An Endevco Model 2110 Impedance Head was used to measure simultaneously the force transmitted to the brass mass and the resulting acceleration. This impedance head contains two piezoelectric crystal transducer elements. One of these acts as a force transducer; the other as an accelerometer. In Fig. 1, the impedance head is shown mounted on a $\frac{1}{2}$-in steel stud between two conically-shaped adapters. The $\frac{1}{2}$-in stud is connected to the drive spindle of the force generator by means of a $\frac{1}{4}$-in stud.

Both the brass cylinder and the vibration generator were suspended from the overhead by means of steel wires. Turnbuckles were used in the suspension system to align the axis of the brass mass with that of the vibration generator.

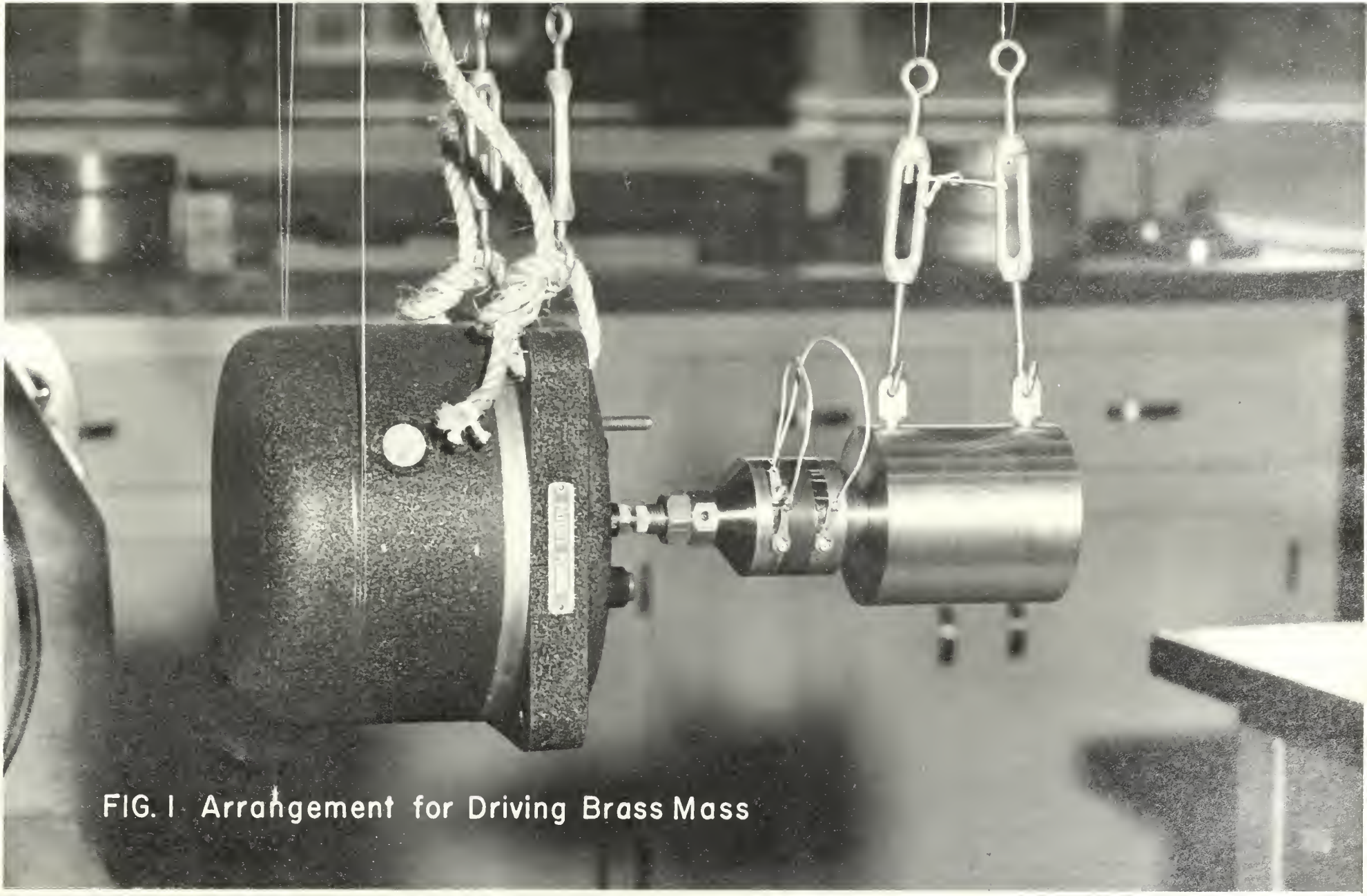

FIG. 1 Arrangement for Driving Brass Mass

2.2 The Cantilever Beam

The beam used in this investigation was a steel beam, the dimensions and properties of which are summarized below:

ℓ = free length (after clamping) = 13.00 in

b = width (distance parallel to neutral axis) = 1.992 in

h = height (distance perpendicular to neutral axis) = 0.501 in

ρ = mass density = 0.282 lbm/in^3

E = Young's modulus = 29.58 x 10^6 psi

2.3 The Clamping Jig

In order to approximate the clamped end condition for the cantilever beam, a clamping jig was designed by the author and manufactured by the Engineering School Machine Shop. This clamping jig is shown assembled in Fig. 2 and disassembled in Fig. 3. It is essentially a vice, the loading of which is provided by a universal testing machine rather than by a power screw as on a machinist's bench vice.

The clamping jig consists of (1) a body or frame which was machined from a single piece of steel, (2) a rectangular base block, (3) two loading blocks which slide vertically within the frame, (4) two clamping blocks which slide horizontally on the base block, and (5) two loading buttons which transmit the load from the crosshead of the testing

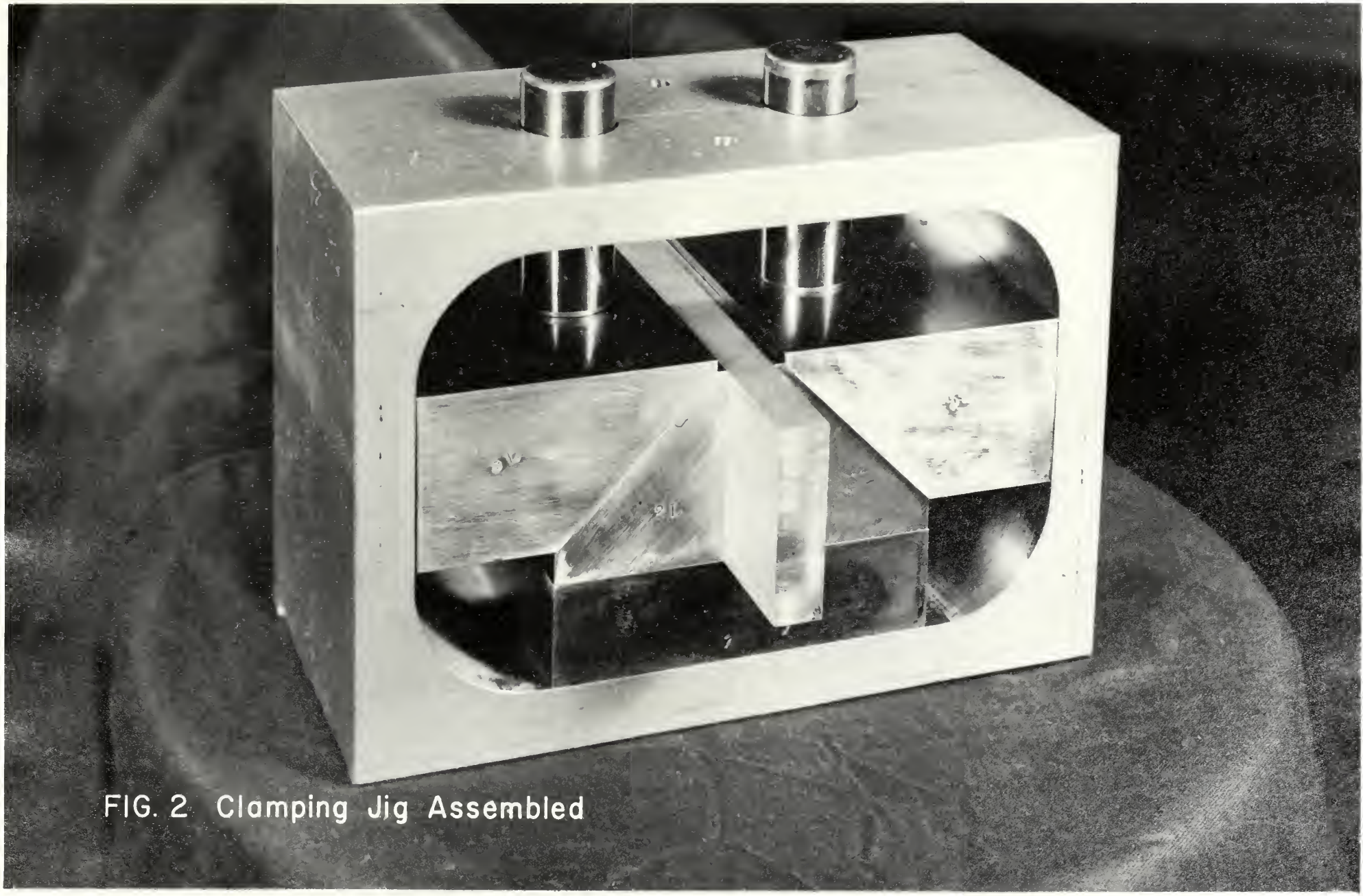

FIG. 2 Clamping Jig Assembled

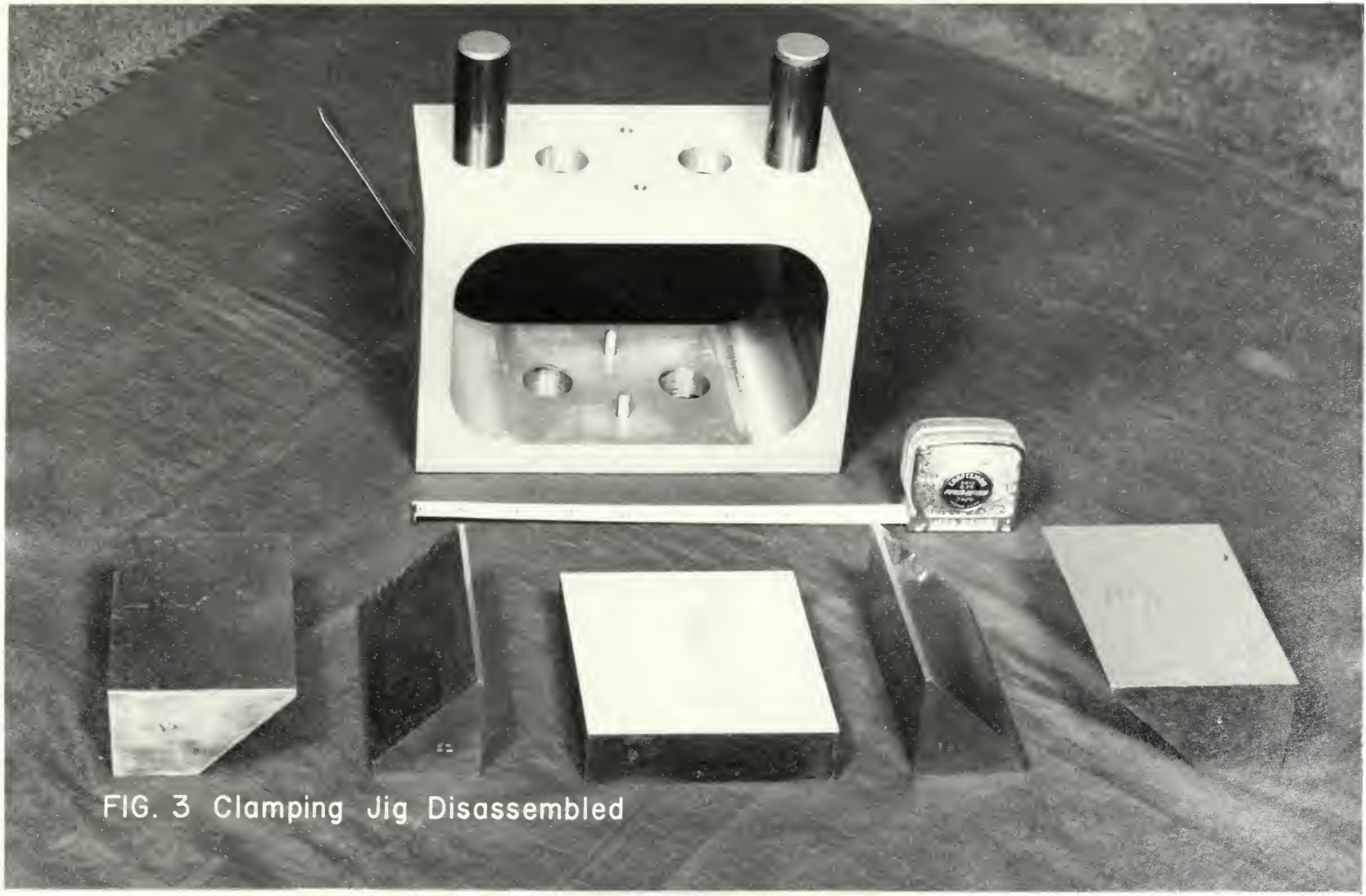

FIG. 3 Clamping Jig Disassembled

machine to the granite blocks.

A load of about 10,000 lbf was used to clamp the end of the cantilever. At a forcing frequency of 100 cps, varying the load from 2,000 to 20,000 lbf had a negligible effect on the observed value of effective mass.

The manner in which the clamping jig was actually used is illustrated in Figs. 4 and 5.

2.4 Cantilever Drive Arrangement

Ideally, in this investigation, it would have been desirable to

(a) drive the beam sinusoidally so that the driving force was always exerted perpendicular to the neutral axis of the beam in its equilibrium position,

(b) without loading the beam by the attachment of any driving member or measuring instruments.

The purpose of the first of the above two requirements is to obtain the postulated sinusoidal excitation. The second is to preserve the nature and hence the response of the structure under consideration, namely a cantilever beam.

There are practical considerations which make it difficult if not impossible to realize either of the conditions indicated above. Very briefly, it is necessary to supply the driving force through some sort of an attachment in order to get a quantitative measure of the driving

force. Attaching anything to the beam alters the character of the structure to be analyzed.

In this investigation two different drive arrangements were used, one a 'direct' drive, and the other an 'elastic hinge' drive.

The direct drive, which is illustrated in Fig. 4, was suggested by one investigator. [16] It is essentially the same arrangement which was used to drive the cylindrical brass mass in the preliminary investigation. (See Section 2.1) One of the adapters was simply screwed into the end of the beam. The reasons for employing this direct drive rather than some other arrangement were that (a) it was simple, and (b) there was reason to believe that the elements in the drive between the impedance head and the beam could be treated as pure masses in correcting the observed effective mass. (It is difficult to evaluate the influence of elements in a drive arrangement which cannot be considered as pure masses.)

The elastic hinge drive, which is illustrated in Fig. 5, was suggested by another engineer [17] as a means of providing for (a) rotation of the point of attachment and (b) protection of the vibration generator against bending moments applied to its drive spindle as a result of this rotation. The details of the elastic hinge drive and of the direct drive are illustrated in Fig. 6. The impedance head, one of the conically-shaped adapters, and the two nuts

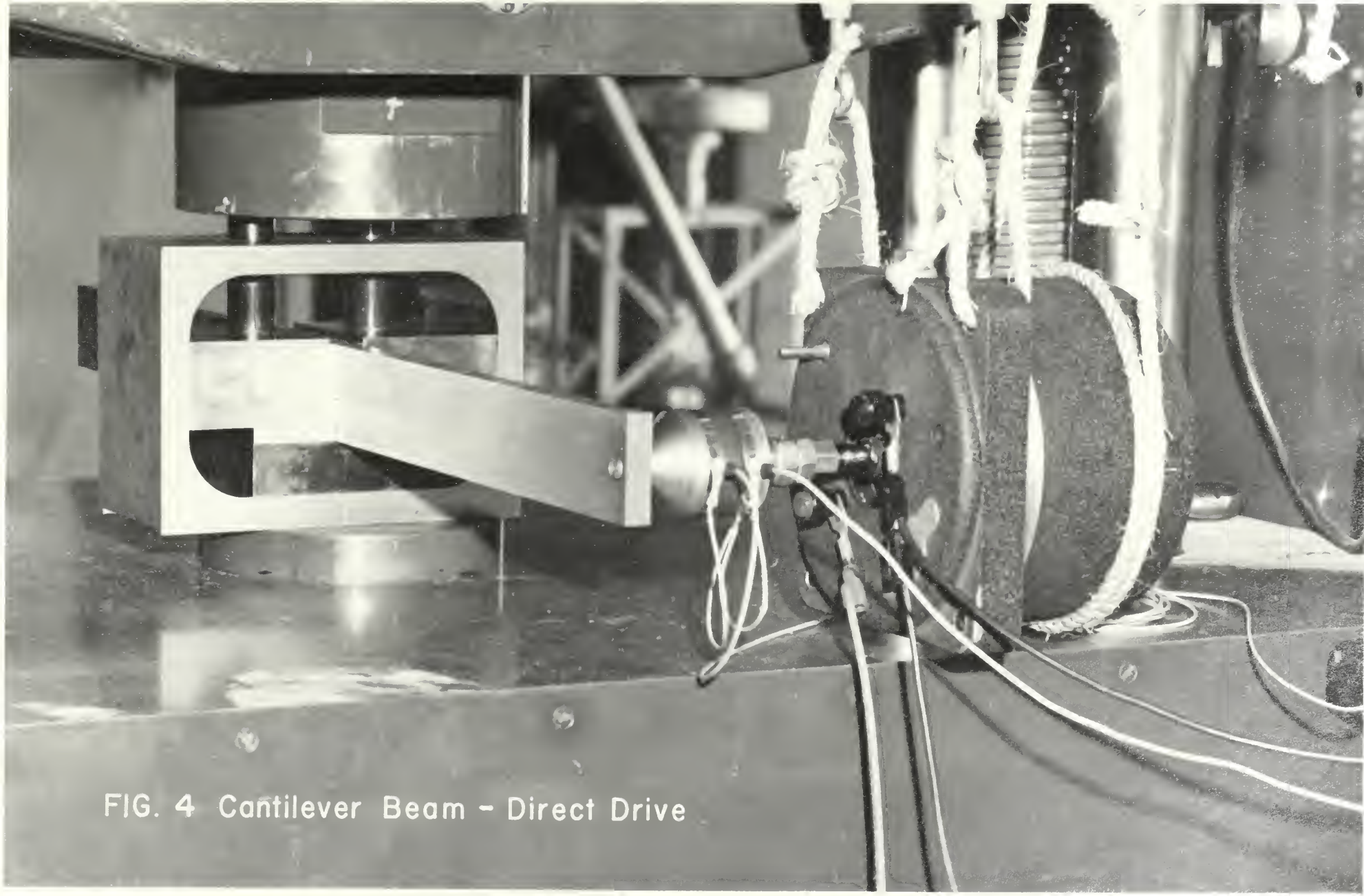

FIG. 4 Cantilever Beam - Direct Drive

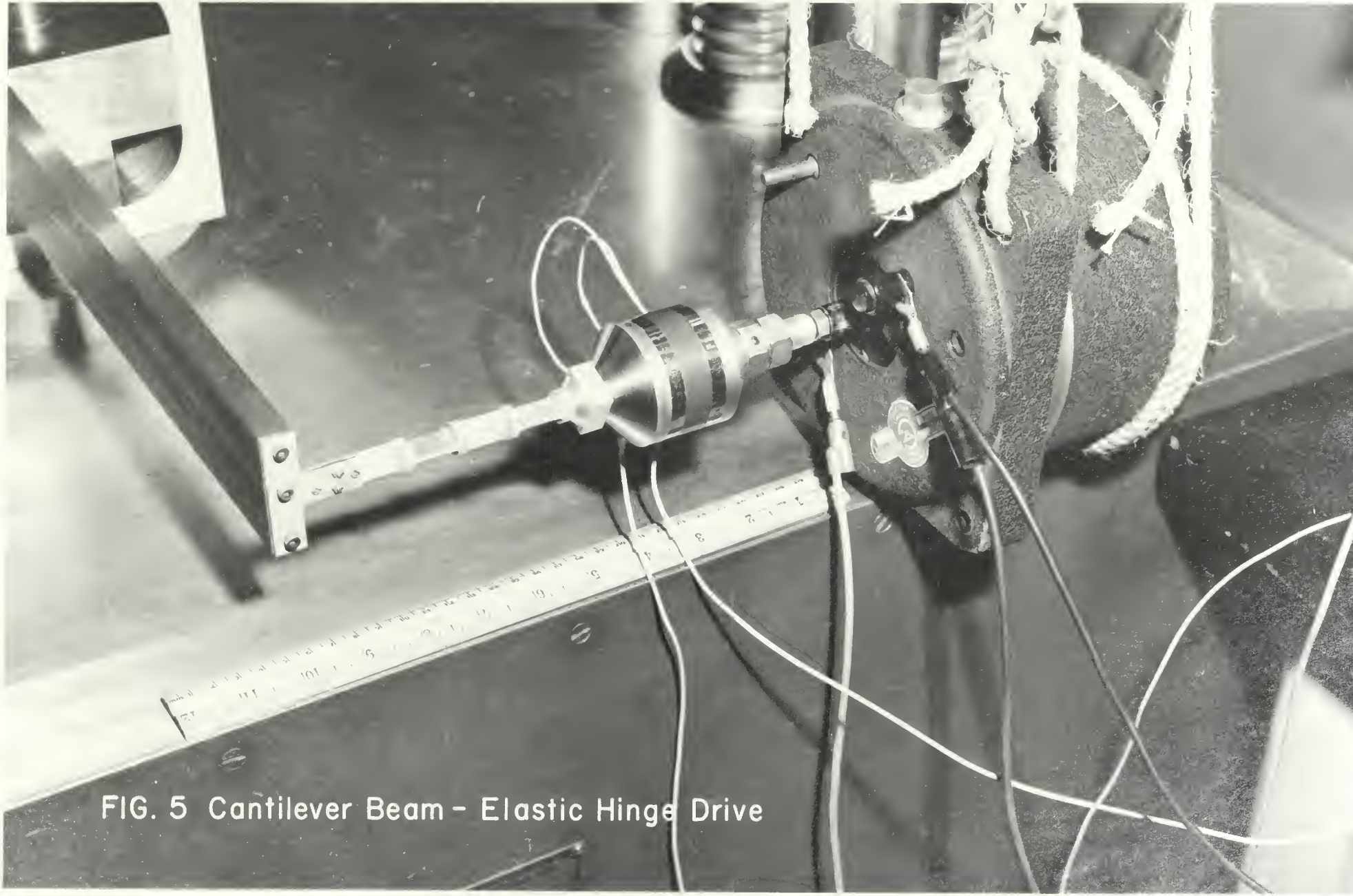

FIG. 5 Cantilever Beam - Elastic Hinge Drive

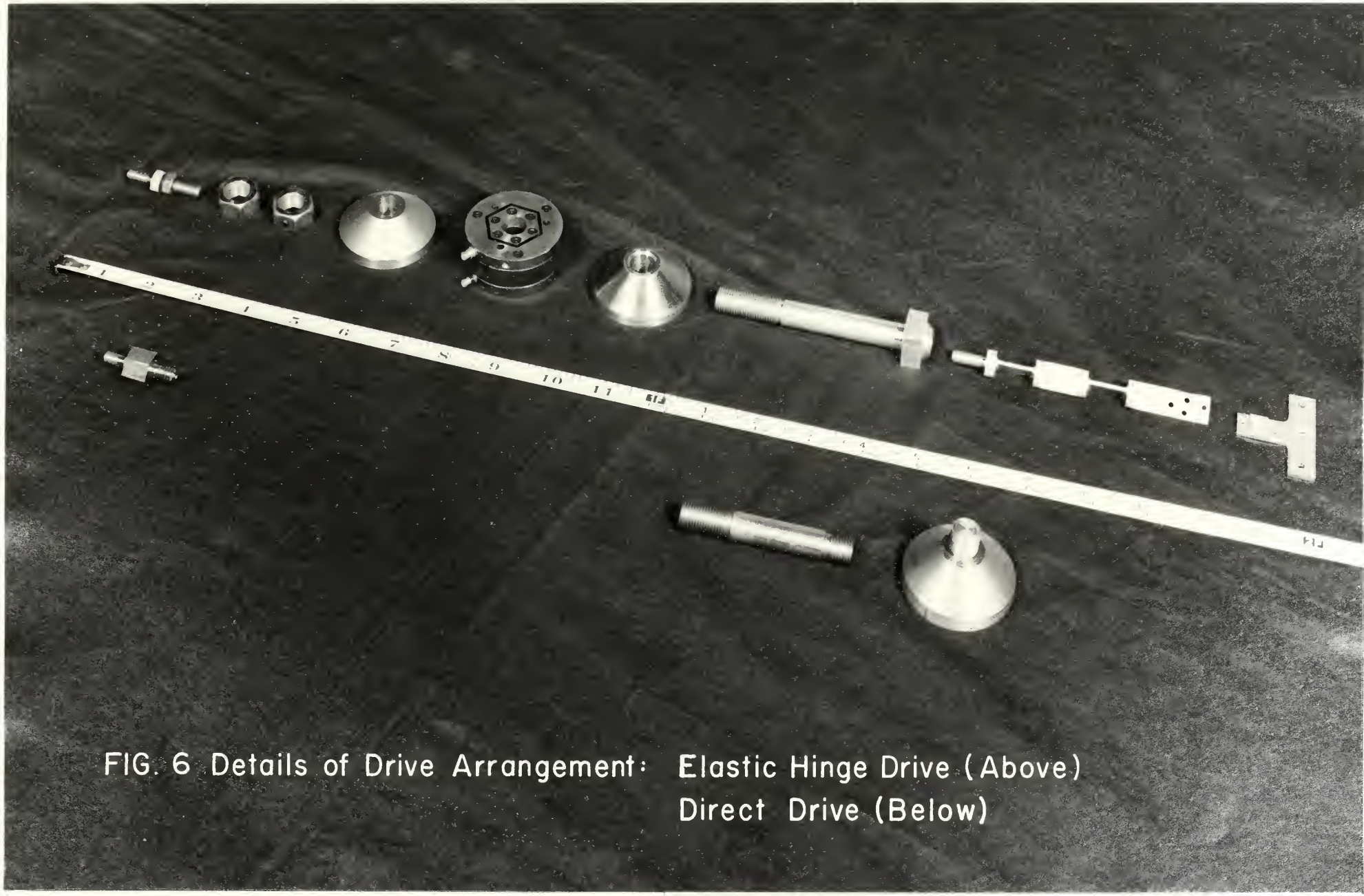

FIG. 6 Details of Drive Arrangement: Elastic Hinge Drive (Above)
Direct Drive (Below)

shown in the upper portion of the figure were also used with the 'direct' drive which is illustrated in the lower part of the figure.

The results obtained using the direct and elastic hinge drives may be found in Sections 3.2, 3.3, 3.4, and 3.5.

2.5 Arrangement for Obtaining Transfer Impedances

As defined in Section 1.2, transfer impedance is the ratio of force to velocity in which these two quantities are measured at different points. Two transfer impedances were determined in this investigation in order to get an indication of the linear behavior of the cantilever. As Bishop points out in reference 14, if the structure is linear,

$$\alpha_{x\ell} = \alpha_{\ell x} \tag{19}$$

That is, the ratio of the displacement at x due to a sinusoidally varying force acting at ℓ should be the same as the displacement at ℓ due to a sinusoidally varying force applied at x. (This is a statement of the familiar reciprocity relation.)

One transfer impedance was obtained by driving at the end of the cantilever, as shown in Fig. 5, and measuring the resulting acceleration at a point four inches from the end of the beam. Force was measured using the impedance head,

and acceleration was measured using an Endevco model 2215 accelerometer. The accelerometer was stud-mounted on an aluminum block having a diameter of 7/8 in and a height of 3/4 in. The aluminum block was attached to the steel cantilever with dental cement.

The second transfer impedance was obtained by driving at a point four inches from the end of the cantilever and measuring the resultant acceleration at the end of the beam. The elastic hinge drive was used, the elastic hinge being attached to the beam by means of an aluminum 'T'. Force was measured with the impedance head and acceleration with the model 2215 accelerometer.

The results of this phase of the investigation may be found in Section 3.5.

2.6 Instrumentation

The equipments used in measuring effective mass in this investigation can be considered as three separate channels of instrumentation - an excitation channel, a force channel, and an acceleration channel.

The excitation channel consisted of those instruments used in exciting the driven structure:

a. Sine wave generator
b. Power amplifier
c. Vibration generator

d. Electronic counter for monitoring the frequency of excitation, and

e. Meters for monitoring the voltage and current to the vibration generator.

The force and acceleration channels were identical and consisted of

a. Transducer (Impedance Head or Accelerometer)

b. Cathode follower

c. Band pass filter

d. Cathode ray oscilloscope for monitoring voltage wave forms

e. Vacuum tube voltmeter for measuring signal voltages.

These three channels of instrumentation are shown schematically in Fig. 7.

In order to determine the phase angle θ between force and acceleration, it was necessary to modify the instrumentation shown in Fig. 7. Two different arrangements were used to measure phase angles, depending on the amount of distortion in the signals. If both V_F and V_a were undistorted, the arrangement shown in Fig. 8 was used. One of the signals was connected to the vertical deflection circuit of a cathode ray oscilloscope and the other signal to the horizontal deflection circuit. Since V_F and V_a were sinusoidal signals of the same frequency, the resulting Lissajous pattern was an ellipse. A simple lag network, which consisted of a variable resistance in series with a variable capacitance, was used to retard one of the

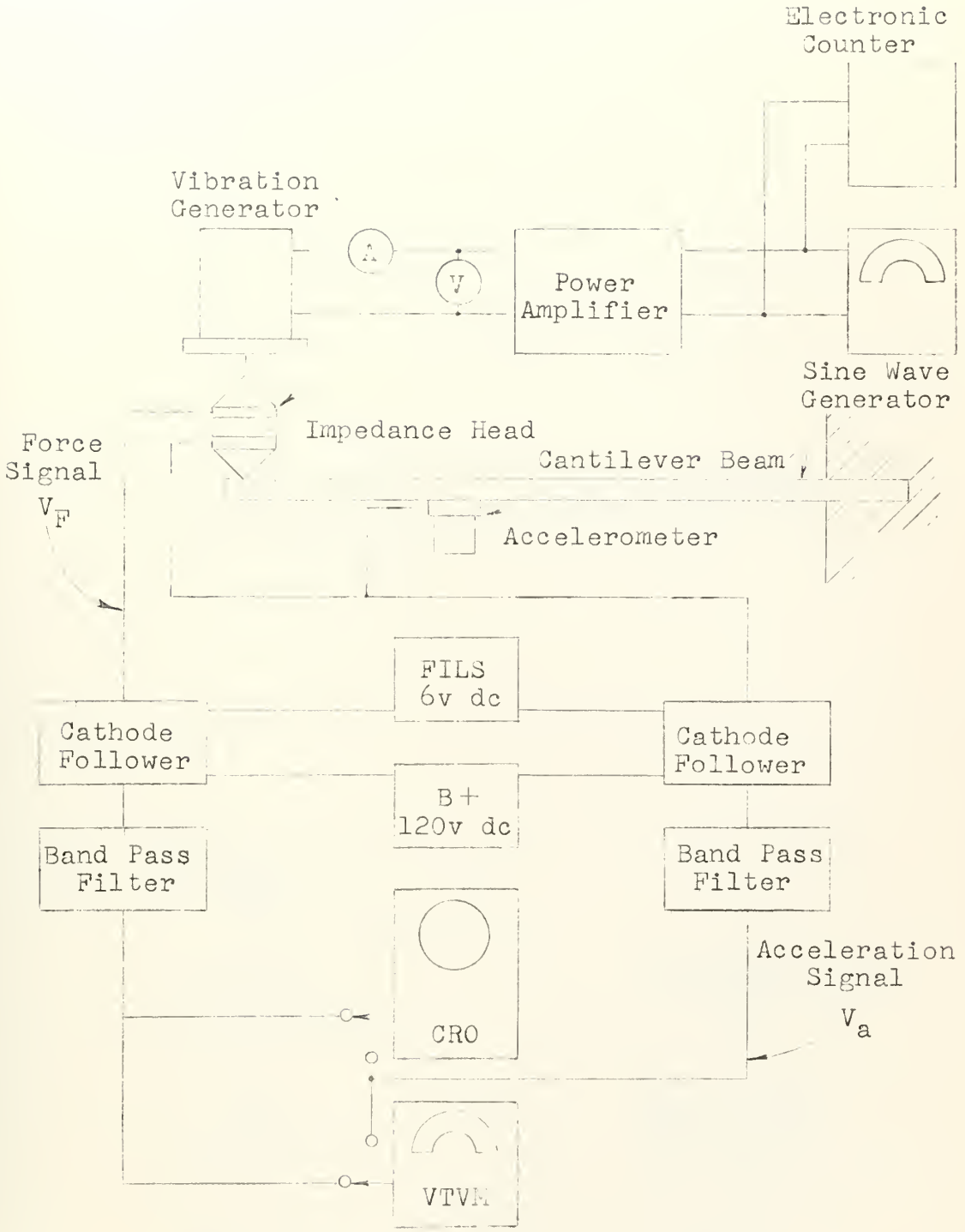

Fig. 7. Block Diagram of Instrumentation for Determining the Magnitude of Effective Mass

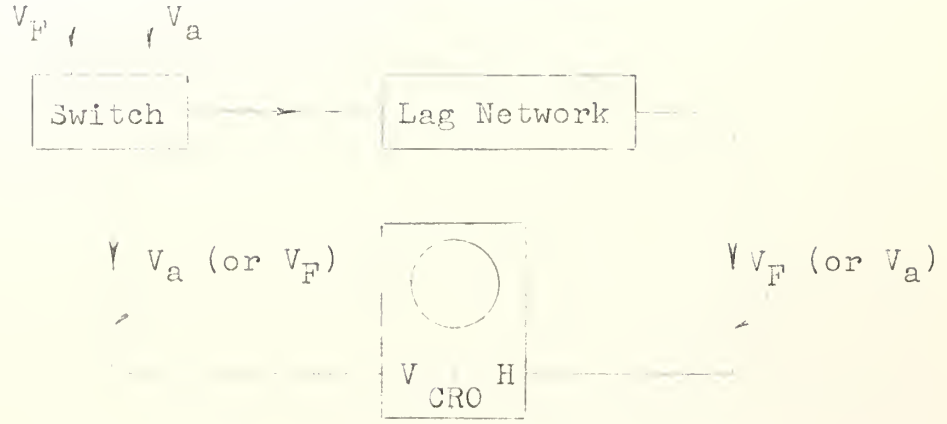

Fig. 8. Block Diagram of Instrumentation for Measuring the Phase Angle θ when Force and Acceleration Signal Voltages are not Distorted

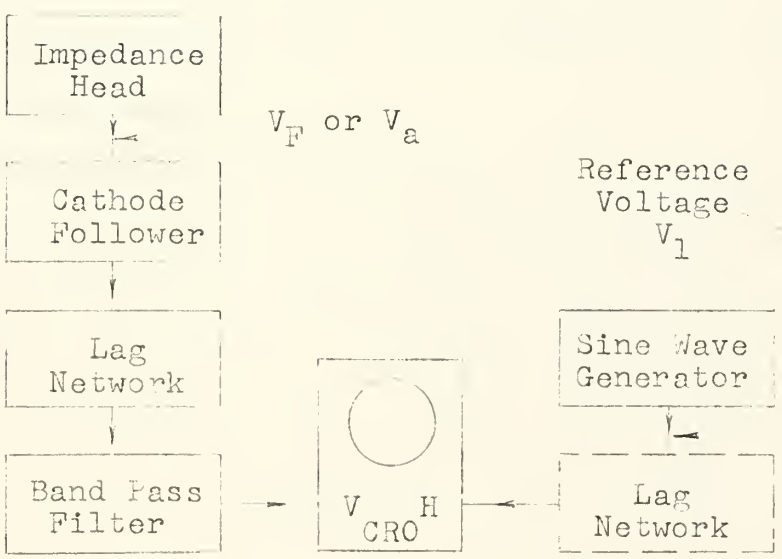

Fig. 9. Block Diagram of Instrumentation for Measuring the Phase Angle θ when Force and/or Acceleration Signal Voltages are Distorted

signals with respect to the other in order to collapse the ellipse to a straight line. The amount of resistance and capacitance inserted determined the angle by which one signal was retarded in order to produce phase coincidence (positive slope of the collapsed ellipse) or phase opposition (negative slope). A schematic diagram of the lag network and the development of the transfer function from which θ was determined is contained in Appendix C. A simple switch was used to select which signal, V_F or V_a, would be retarded.

When either or both of the signals from the impedance head were distorted, it was necessary to resort to a similar but more tedious method for determining θ. The equipment arrangement for this alternate procedure, which is shown in Fig. 9, includes a band pass filter to eliminate the offending higher frequency components in the signal from the transducer.

The procedure for measuring phase angles was similar to that outlined above for the arrangement shown in Fig. 8. However, in this case, two phase angles were determined at each frequency of vibration - one phase angle between V_F and a reference voltage V_1 and another phase angle between V_a and V_1. It was then necessary to compare these two phase angles to determine θ, the phase angle by which force led acceleration.

A complete list of the instrumentation used in this investigation is contained in Appendix A.

3. Results and Discussion of Results

3.1 Preliminary Investigation

The arrangement for supporting and exciting the cylindrical brass mass used in the preliminary investigation was described in Section 2.1. This mass was vibrated in order to gain familiarity with the instrumentation and to determine the validity of a number of theoretical relationships. If the impedance head and the means of attaching it to the brass cylinder act as a pure mass, being perfectly rigid, the observed effective mass of the brass cylinder corrected for the mass of the driving structure between the impedance head and the cylinder should be equal to the actual mass of the cylinder. (See Appendix D.) The effective mass so determined should be a constant function of frequency. Furthermore, the sinusoidal acceleration of the mass should be in phase with the sinusoidal driving force.

The results of this preliminary investigation are shown graphically in Fig. 10, where both effective mass and phase angle are plotted as a function of the exciting frequency. The effective mass of the brass cylinder is essentially constant from 15-1000 cps. Above 1000 cps it increases until an antiresonant peak is reached at 3600 cps. The effective mass then decreases rapidly toward a resonance which presumably occurs above 10 kc.

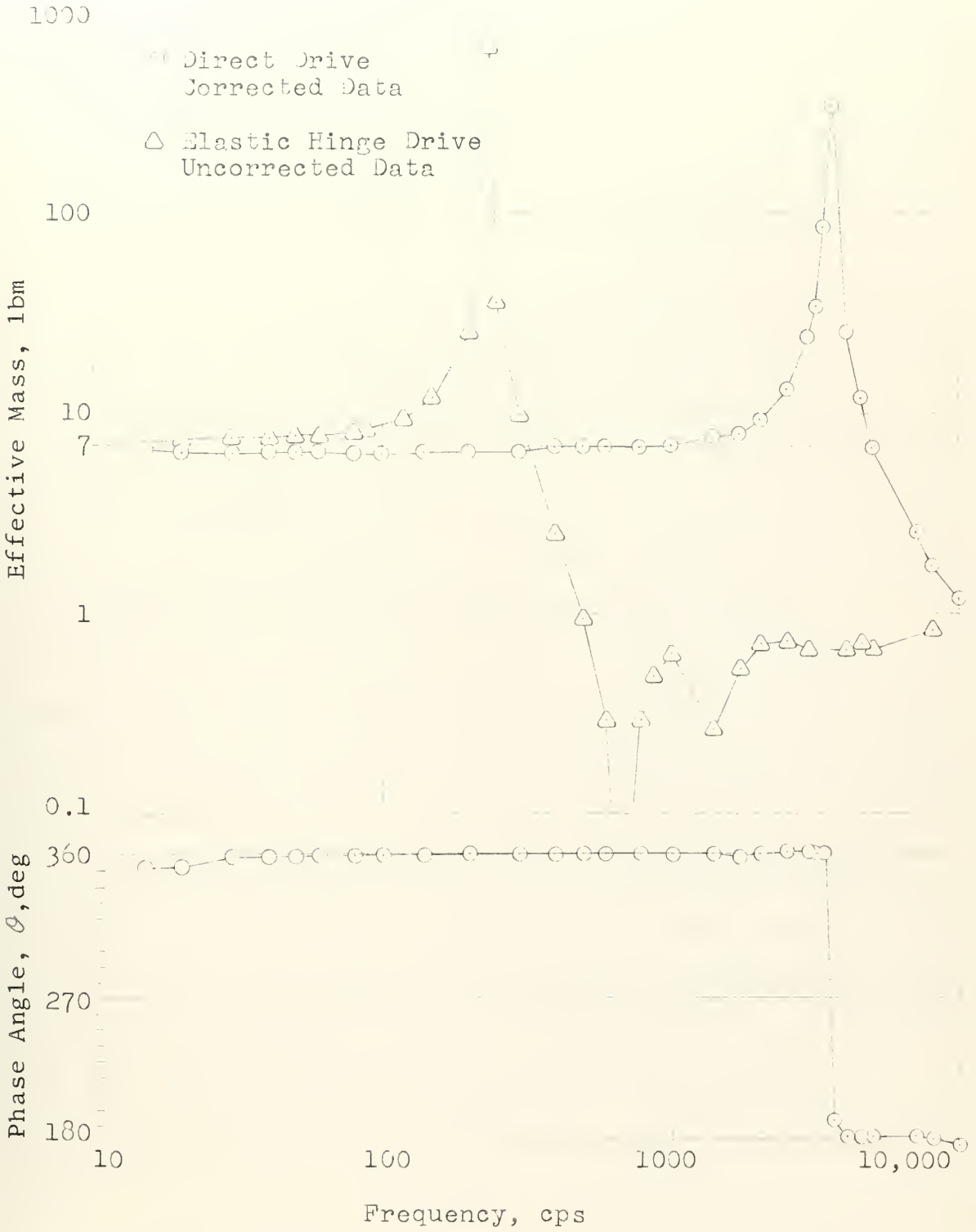

Fig. 10. Effective Mass and Phase Angle as a Function of Frequency. Longitudinal Vibration of a Cylindrical Brass Mass. m = 6.99 lbm.

In the lower portion of Fig. 10, θ is plotted to the same frequency scale as observed effective mass. θ is essentially zero from 10 cps to the 3600 cps antiresonant peak at which it changes abruptly to approximately 180°. If there had been a resonant frequency below 10 kc, theoretically the phase angle would have shifted from 180° to 0° at that frequency. Although a resonant 'valley' was not observed in this preliminary investigation, this pattern of phase angle shifts was observed when a cantilever beam was vibrated. (See Section 3.3.) The rate at which the phase angle changes with frequency gives a qualitative indication of the amount of damping in the system. A relatively small amount of damping is indicated by an abrupt change such as that shown in Fig. 10. If there had been more damping in the system, the change would have been more gradual.

The average value of the effective mass of the brass cylinder below 1000 cps is about 6% less than the mass of the cylinder as determined by weighing. The 6% discrepancy noted here indicates the order of magnitude of the experimental error which may be anticipated when exciting small structures with this drive arrangement and this impedance head.

The antiresonant peak at 3600 cps in Fig. 10 is considered to be an antiresonant frequency of the brass mass, and the impedance head - adapter 'package' considered as a

system. The phase angle θ changes from 0° to 180° in the vicinity of the antiresonant 'peak' indicates that the impedance which the impedance head 'sees' changes from an impedance which is 'mass-like' below 3600 cps to one which is 'spring-like' above that frequency. Thus, it appears that, in addition to the mass effects which were anticipated, there is a stiffness in the brass cylinder-impedance head system which influences the observed effective mass above 1000 cps.

Vibration of the impedance head - adapter 'package' separately indicated that the antiresonant 'peak' observed in Fig. 10 was not due to an antiresonance in this 'package', or subsystem. Observation of force, acceleration and the phase angle between force and acceleration established that this 'package', by itself, does act as a pure mass from 30 cps to 10,000 cps. Although the observed effective mass of this 'package' varied between 0.730 and 0.787 lbm between 30 cps and 7000 cps and increased to 0.950 lbm at 10,000 cps, the phase angle θ was essentially zero throughout the observed frequency range.

This illustrates the difficulty of measuring experimentally the impedance of a pure mass. The necessity of physically exciting the mass and of measuring force and velocity (acceleration in this case) requires the attachment of some means of driving the mass and measuring the resultant motion. Once these attachments have been made,

the structure (and hence its response to an exciting force) has been changed. This is illustrated very effectively in Fig. 10. The same problem was encountered in determining driving point and transfer impedances of a cantilever beam.

The significance of the curve (Fig. 10) obtained using the elastic hinge drive is explained in Section 3.4.

The results illustrated in Fig. 10 are similar to those obtained by other investigators who used this method as a check on the accuracy of their experimental procedures. [11]

3.2 Cantilever Beam - Direct Drive

The arrangement for exciting the cantilever beam by means of the direct drive is described in Section 2.4 and illustrated in Fig. 4.

The results of exciting the beam in this manner are shown graphically in Fig. 11. The lower of the two curves was obtained using Bishop's receptance function which is discussed in Section 1.4. Equation (14) was used as the basis for the computer solution for effective mass as a function of frequency. Appendix B is the computer program which was used to calculate the points from which the 'theoretical' curve was plotted. This then provides the theoretical function with which the experimentally-derived impedance function is compared.

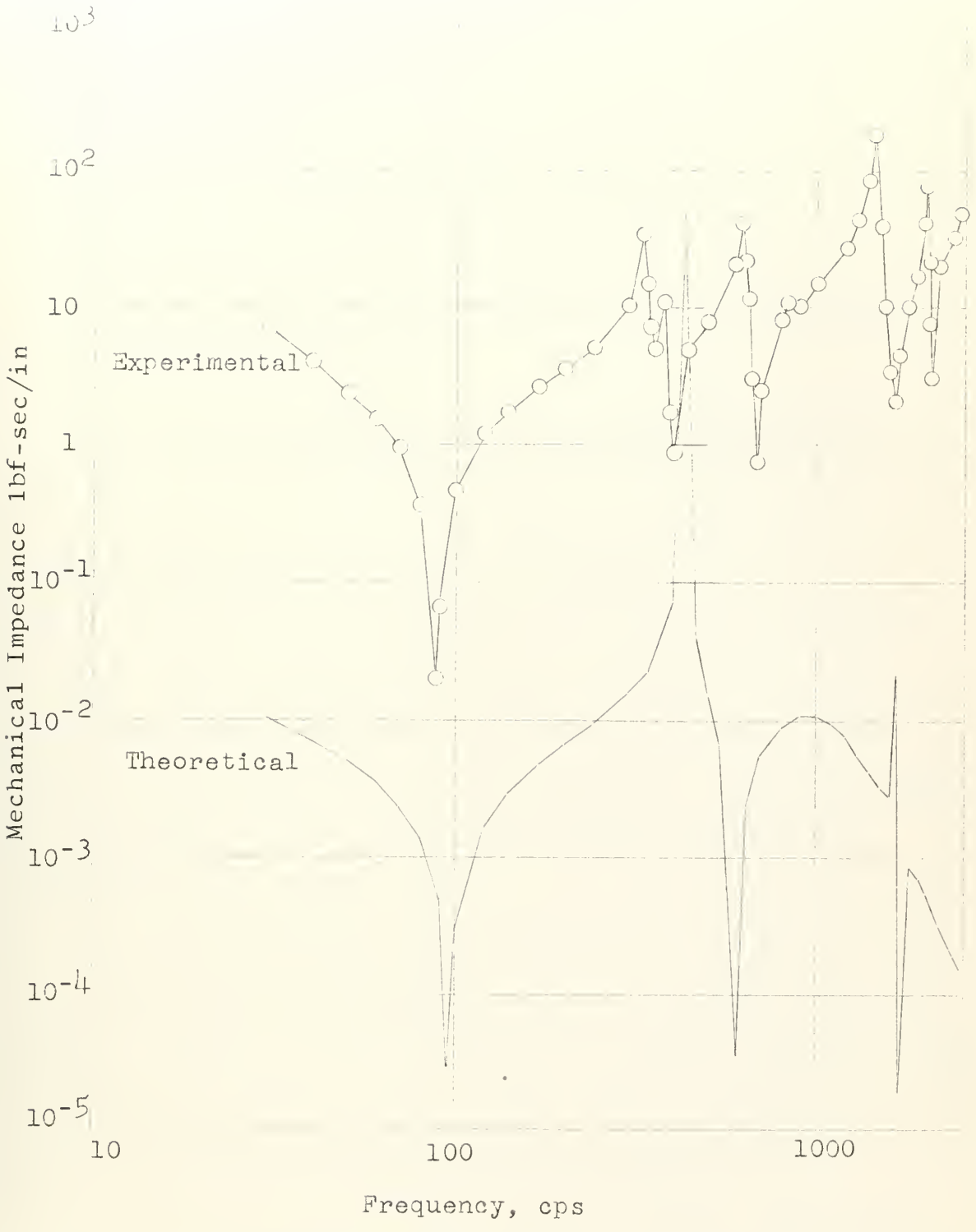

Fig. 11. Driving-point Impedance as a Function of Frequency. Tip-driven Steel Cantilever Beam, 13 in x 2 in x 0.5 in. Direct Drive. Comparison of Experimental Results with Theoretical Function.

In attempting to correlate the experimental impedance function in Fig. 11 with the theoretical function, a number of features of the curves become evident:

a. The general shape of the curves,

b. The vertical displacement between the two curves,

c. The greater number of resonances and antiresonances in the experimental curve,

d. The difference in frequency at which corresponding resonances (or antiresonances) occur on the two curves, and

e. The good correspondence between the two curves at the first antiresonant frequency.

These features will be discussed in succeeding paragraphs of this section. The experimental curves obtained using the direct drive (Fig. 11) and the elastic hinge drive (Fig. 13) are similar in several respects. Therefore, some of the remarks in the following discussion may also be considered under Section 3.4.

One feature of the experimental curves in Figs. 11 and 13 is the manner in which the resonant 'valleys' and anti-resonant 'peaks' alternate. This is a general characteristic of impedance curves. The 'valleys' occur at frequencies at which the impedance of the structure (and hence its resistance to motion) is low. These 'valleys' correspond to resonant frequencies of the vibrating system. The 'peaks' occur at frequencies at which the impedance of the structure is high. Therefore, they correspond to antiresonant

curve and the theoretical curve in Fig. 11 may be explained by

(1) the necessity of correcting observed values of effective mass and phase angles,

(2) the accuracy with which these quantities can be measured, and

(3) the 'different structures' concept (presented below).

Practically speaking, the impedance head used in this investigation measures the effective mass of the structure beyond the middle plane of the impedance head. In order to determine the effective mass of the cantilever beam, (or the brass cylinder in the preliminary investigation,) it was necessary to apply to the observed effective mass a correction to account for the effective mass of the accelerometer end of the impedance head, the adapter and part of the $\frac{1}{8}$-in mounting stud. The manner of making this correction is outlined in detail in Appendix D (Sample Calculations). Reference to equation (4-D) in Appendix D indicates the vector nature of the correction method. Very briefly, the effective mass of the impedance head - adapter 'package' must be subtracted vectorially from the observed effective mass. Thus, the effective mass of the beam, by itself, is a vector difference. Since the correction to be applied to the observed effective mass is approximately

0.7[illegible] lbm. and the smallest values of observed effective mass are of the same order of magnitude, it is apparent that the smallest value of the difference between them (vector or algebraic) is about 0.0[illegible] or 10^{-3} lbm. The effective mass at the first computed resonance in Fig. 11 is about 10^{-5} lbm and, at the third computed resonance, 10^{-6} lbm.

With the instruments used in this investigation and the values of transducer sensitivities provided by the manufacturer, measurement of voltages V_F and V_a to three significant figures is about the best accuracy which may be expected.

Thus, the limitations imposed by the instrumentation preclude a precise correlation of effective mass magnitudes. Effective mass coordinates are not indicated in Fig. 11; but it is interesting to observe that all points on the theoretical curve above 528 cps have ordinates (effective mass) less than 10^{-3} lbm!

The above discussion assumes that phase angles between force and acceleration signal voltages can be determined with the same accuracy as the voltage measurements. Unfortunately, the phase angle measurements were even less precise than the voltage measurements. (A detailed discussion of the procedure for measuring phase angles and the accuracies of these determinations is the subject of Section 3.3.) The inherent limitations of the procedures

and equipment for measuring phase angles make good correlation of the two curves in Fig. 11 even more unlikely.

Thus, it may be observed that, in general, the correlation between experimental and theoretical values of impedance (effective mass) in this investigation is valid qualitatively but not quantitatively.

In comparing the experimental and the theoretical curves in Fig. 11, it is important to bear in mind that they represent impedance functions for different structures. The lower (theoretical) curve describes a mathematically-defined cantilever beam. For this beam, at the 'built-in' or 'clamped' end, the displacement and the slope are always zero. At the 'free' end, both bending moment and shear are zero, as developed in elementary strength of materials. The upper (experimental) curve describes an approximation to the mathematically-defined cantilever beam, and herein lies one of the principal reasons for the difference in the appearance of the two curves.

In practice, the cantilever beam used in this investigation only approximated the mathematically-defined cantilever for the following reasons:

1. Although the clamping jig worked very well, it did not terminate the beam in an infinite impedance (as it should have done ideally). When vibrating at the first resonant frequency, even with modest power input to the vibration generator, the whole testing machine, by means of which the

clamping [illegible] vibrated [illegible]. And the testing machine is a rather massive structure.

2. With the direct drive, the cantilever was driven at a point about 0.400 in from the end of the beam. The manner of attaching the impedance head 'package' to the beam was the controlling factor in selecting the driving point. One of the adapters was simply screwed into the end of the beam. (See Section 2.4 and Fig. 4.) The distance from the clamping blocks to the center line of the threaded portion of the adapter was 13.00 in. Thus, the free length of the beam was about 13.40 in. The theoretical curve is based on a free length of 13.00 in. In addition to the difference in lengths, it is also apparent that the physical structure represented by the experimental curve is not a tip-driven cantilever. The driving point is actually inboard of the end of the beam about 0.400 in.

3. Attaching the impedance head 'package' and the vibration generator to the end of the beam was necessary in order to excite the beam and to measure both the exciting force and the resultant motion. However, by so doing, the freedom of motion of the end of the beam and the very nature of the structure were modified. This is very important. The manner in which the attachment of this driving-measuring structure affects the response of the driven structure is clearly indicated in the results of the preliminary investigation (Section 3.1) in which a mass

experiment [illegible].

4. The vibration generator and the impedance head 'package' were rigidly attached to each other and to the end of the beam. (See Fig. 4.) The consequence of such an attachment was that the sinusoidal exciting force was always exerted perpendicular to the end of the beam. The theoretical curve is predicated on application of the exciting force perpendicular to the neutral axis of the beam in its equilibrium position. One of the practical consequences of this drive arrangement was a rather violent lateral vibration of the vibration generator at frequencies below 28 cps due to the rotation of the end of the beam.

The greater number of resonances and antiresonances in the experimental curve and the difference in frequencies at which corresponding resonances and antiresonances occur on the two curves may be explained by the 'different structures' discussion presented above. When additional elements are added to a vibrating system, the number of degrees of freedom and the number of natural frequencies of the system are increased.

Even though the nature of the structure has been changed, there are well-defined resonances and anti-resonances in the experimental curve in Fig. 11 which correspond to the resonances and antiresonances in the theoretical curve. This correlation is summarized in the following table.

	Theoretical	Experimental
First resonance	90 cps	89 cps
First antiresonance	424	315
Second resonance	604	586
Second antiresonance	1671	1446
Third resonance	1699	1650

Table 1. Comparison of Experimental and Theoretical Frequencies of Resonance and Antiresonance. Tip-driven Steel Cantilever Beam. Direct Drive. See Fig. 11.

At the first resonance, the frequency correlation is good. At the first antiresonance, there is very good correlation between the impedance magnitudes on the two curves. This is particularly significant because this is the one frequency at which the theoretical curve penetrates the domain of the experimental curve. Good correlation at this point lends credibility to the method of measuring the impedance and the accuracy of the measuring instruments.

3.3 Phase Angle Determinations - Direct Drive

The phase angle data presented in this section are those obtained by exciting the cantilever beam described in Section 2.2 with the direct drive illustrated in Fig. 9. While the data pertain only to the cantilever beam, the accompanying discussion pertains to phase angle determinations in general, using the instruments and equipment

beam excited at its free end using the 'direct' drive arrangement described in Section 2.4. The phase angles in Fig. 12 are 'corrected' phase angles. That is, the observed phase angles have been corrected to account for the effective mass of the impedance head - adapter combination. The phase angle data shown in Fig. 12 must be considered with the experimental impedance magnitude data shown in Fig. 11 to get a complete picture of the experimentally-determined impedance of this cantilever beam. (It will be recalled that both magnitude and phase angle information are required for the complete specification of impedance.)

An examination of Figs. 11 and 12 indicates that the phase angle ϕ does, in fact, change from 270° through 0° to 90° in the vicinity of a resonance, as impedance theory predicts. [5] The rapid rate of change of ϕ with frequency in the vicinity of a resonance or antiresonance confirms qualitatively the validity of the assumption of negligible damping.

The phase angle ϕ is 270° only at frequencies below the first resonance. At frequencies between each anti-resonance and the next succeeding resonance, the phase angle only approaches 270°. This is due to the 'sharpness' of the resonances and antiresonances, and the manner in

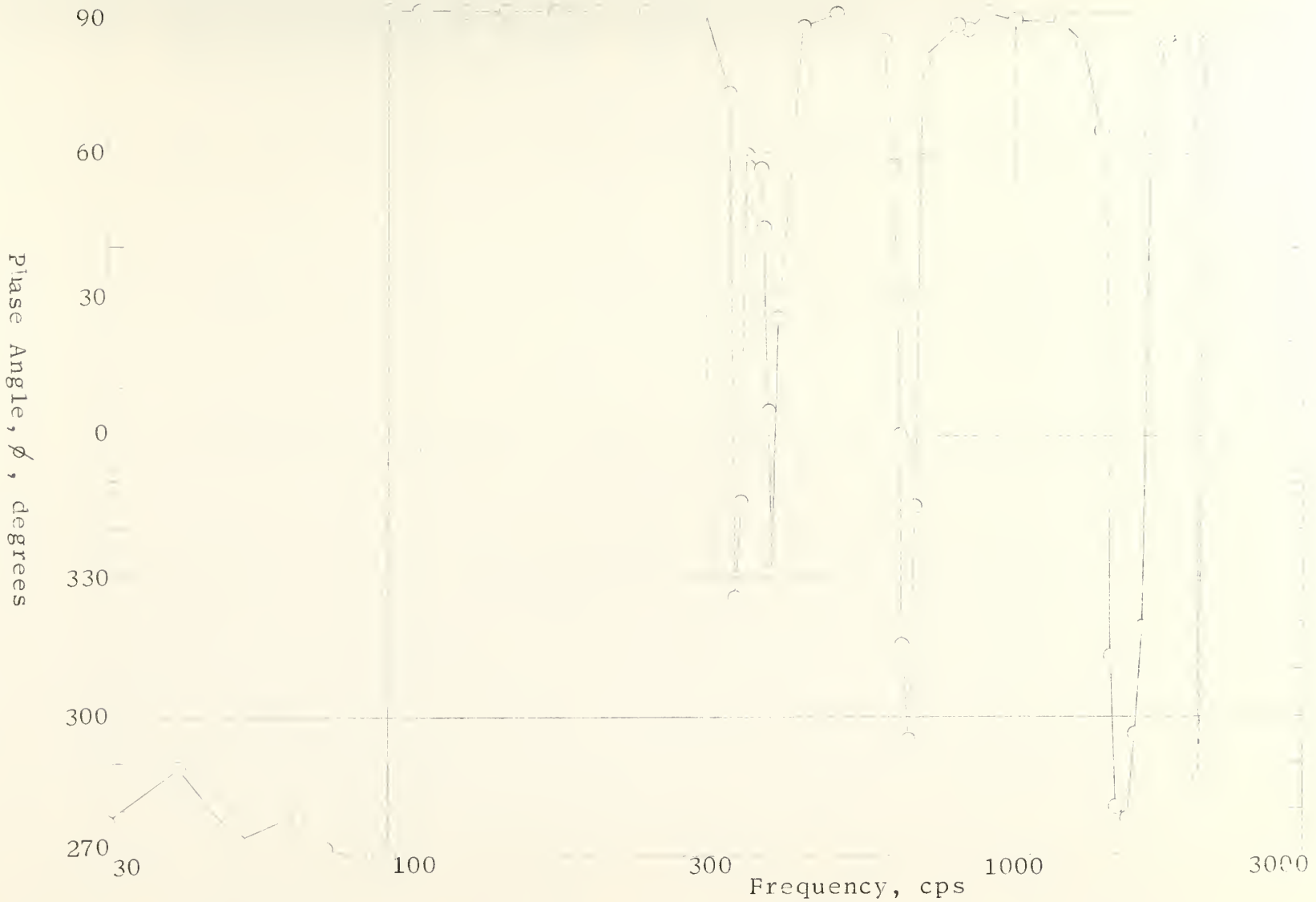

Fig. 12. Phase Angle ϕ vs Frequency. Tip-driven Steel Cantilever Beam, 13 in x 2 in x 0.5 in. Direct Drive.

[illegible] follows hard on the heels of the [illegible] discontinuance.

The phase angles plotted in Figs. 10 and 12 appear to be reasonably well-behaved. However, appearances are deceptive. The phase angle data in this thesis investigation were the least precise of all the data taken. Since the corrected magnitudes of impedance (or effective mass) are dependent on the phase angle, lack of precision in determining these phase angles reduces the accuracy with which impedance magnitudes may be reliably determined. In succeeding paragraphs, the procedures used for obtaining and reducing phase angle data will be discussed. Suggestions are also included for subsequent investigations.

The instrumentation and procedures used in determining phase angles in this investigation are described in Section 2.6. Figs. 7, 8 and 9 are block diagrams which illustrate the equipment arrangements used. A list of equipment and instruments used in this thesis is contained in Appendix A. A detailed derivation of the equations for determining phase angles may be found in Appendix B. Sample calculations of phase angles, using both equipment arrangements described in Section 2.6, are included in Appendix C.

As indicated in Section 2.6, the procedure for determining phase angles was a point-by-point procedure. Phase angles were not determined continuously, but at selected frequencies at which effective mass data had been taken.

[illegible] different frequencies were [illegible] must be added [illegible] the phase angle curve in Fig. [illegible] and a similar number for the curve in Fig. 12. The procedure involved was a slow and tedious one. The 'direct' method, using the equipment arrangement shown in Fig. 8, required less than half the time required by the 'indirect' procedure illustrated in Fig. 9. However, the indirect method is considered the more accurate of the two procedures. If the procedures were sufficiently accurate, they would be satisfactory for determining small numbers of phase angles at particular frequencies. When it is desired to determine a large number of phase angles, the procedure and the instrumentation are considered unsatisfactory.

The phase angle procedure, in addition to being slow, left much to be desired as far as accuracy is concerned. Using the direct method, it is estimated that α (equation (3-3)) can be determined within 1° when α is less than 5°; within 2° when α is between 5° and 10°; and within 5° when α is between 10° and 30°. Values of α greater than 30° so determined are considered to be of questionable accuracy. As α approaches 90°, the value of ωRC approaches infinity. At a given frequency then, the product of R and C must approach infinity. This consideration indicates the difficulty of determining the value of α experimentally when α approaches 90°. This difficulty was actually experienced. At frequencies in the vicinity of

a [illegible] ce, with R held constant, a minimum value of C could be found to collapse the ellipse. However, increasing C beyond this value would not produce an elliptical Lissajous pattern as it would for small values of α. Thus, at near-resonant or-antiresonant frequencies, C and ωRC were indeterminate, and it was necessary to use the indirect method of determining these phase angles.

Although, the indirect method involved determining two values of θ for each value of θ, it is considered the more accurate of the two phase angle procedures. It was used whenever V_F or V_a was distorted, when C was indeterminate using the direct approach, or when there was some other reason to question the value of α determined directly. It is difficult to even estimate the accuracy of this method. Some generalizations are possible, however. It is subject to the same limitation as the direct method when the angle between V_F (or V_a) and the reference voltage V_1 approaches 90°. Otherwise, the accuracy of phase angles so determined appears to be constant and within about $2\text{-}3^\circ$. Once again, however, this figure represents only an educated guess.

The calculations contained in Appendix D indicate the difference in values of θ obtained using the direct and indirect methods. The frequency selected for these sample calculations is one at which a relatively large difference was obtained. When θ was determined at other frequencies

using both procedures, the differences were frequently small, of the order of 0.1°.

Equation (3-3) in Appendix 3 was the basic equation used in reducing phase angle data. The use of this equation and the lag network shown schematically in Fig. 1-3 was based on the assumption that the resistances and capacitances introduced by this lag network would be large compared to other resistances and capacitances in the measuring circuits. The observations made below give cause to doubt the validity of this assumption.

Theoretically, the value of R_3 required to produce phase coincidence or phase opposition at a given frequency should be a constant. Such was not the case in practice. Table 2 indicates one example where this condition was observed. These data were taken when driving the cantilever beam with the elastic hinge drive arrangement at 1000 cps. All of the angles were small, but the variation in $\omega R_3 C_3$ is considerable. In order that the results obtained would be reasonably consistent, $R_3 = 1000$ ohms was used whenever the ellipse could be collapsed with this value of resistance.

		0.000314	
		0.00314	0°01'
		0.0314	0°11'
		0.251	1°26'
		0.628	3°36'

Table 2. Variation of ϕ ($\phi = \arctan \omega RC$) in Determining Phase Angles Directly with Different Values of Resistance in Lag Network. 13 in Steel Coil Lever Arm. Elastic Hinge Drive. f = 1000 cps.

In the beginning, the phase angle measurements made by direct projection using a commercial phase meter were [illegible] unsatisfactory. [19] An electronic phase shifter circuit was developed at the Navy Electronics Laboratory for determining phase angles in mechanical impedance investigations pursued by that laboratory. [20] The accuracy of this phase shifter is reported to be better than plus or minus one degree. Use of such a phase shifter in future impedance investigations is recommended.

4.4 Elastic Hinge Drive

The elastic hinge drive, which is illustrated in Fig. 4, was discussed briefly in Section 2.4.

The results obtained using this drive arrangement are illustrated graphically in Fig. 13. Fig. 13 is similar to Fig. 11 in many respects. Discussion of features of the two experimental curves which are similar is contained in Section 3.2. It will not be repeated in this section.

One basic difference between the two experimental curves should be emphasized, however. The experimental curve in Fig. 11 was plotted using corrected values of effective mass. The values used in plotting effective mass in Fig. 13 were uncorrected. Uncorrected values were used in Fig. 13 because

(a) an examination of the observed data suggested that the impedance head - elastic hinge system could not be treated as a pure mass in correcting the observed effective mass, and

(b) there was some question as to how the observed effective mass should be corrected if the behavior of the impedance head - elastic hinge system was, in fact, 'spring-like' at certain frequencies.

In order to determine if the elastic hinge could be treated as a pure mass in correcting the observed values of effective mass, the cylindrical brass mass described in

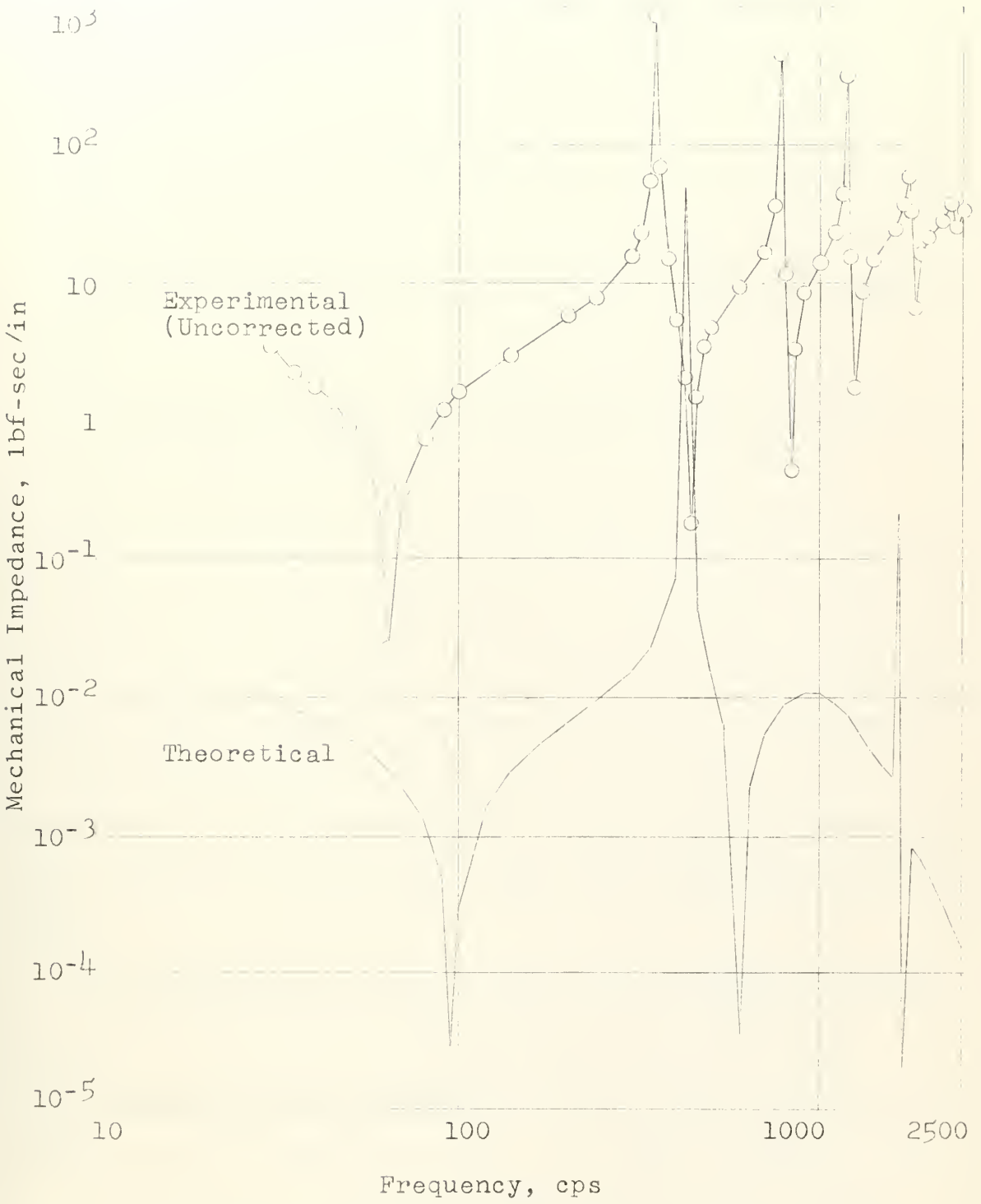

Fig. 13. Driving-point Impedance (Uncorrected) as a Function of Frequency. Tip-driven Steel Cantilever Beam, 13 in x 2 in x 0.5 in. Elastic Hinge Drive. Comparison of Experimental Results with Theoretical Function.

[illegible] using the elastic hinge in lieu of [illegible] The results of this test, which are [illegible] in Fig. 10, illustrated dramatically that the elastic hinge was not acting like a pure mass at all. Therefore, observed values of effective mass were plotted in Fig. 13 with no attempt made to correct them. Theoretically, a transfer impedance function for the impedance head - elastic hinge system could be determined which would make it possible to correct the observed effective mass data. This transfer function could be derived theoretically by considering the impedance head, the adapter and the mounting stud as a pure mass and the elastic hinge as a spring. Or a transfer function could be derived experimentally by measuring force and acceleration at the impedance head, (which poses no problem,) and also measuring force and acceleration at the end of the elastic hinge, (which is a formidable task from a practical point of view.)

The experimental curve in Fig. 13 is similar in shape and in the number and location of resonances and anti-resonances to the corresponding curve in Fig. 11. In general, it is a smoother curve. Its shape resembles that of the theoretical curve up to and including the second resonance of the beam better than does the experimental curve of Fig. 11. However, the height of the first anti-resonant peak gives reason to question the results obtained

ative purposes.

eliminate the lateral vibration at low frequencies as anticipated. If a method could be found to correct for the behavior of the elastic mount, or that better quantitative results could be obtained, there is much to recommend its use in an investigation such as this.

3.5 Transfer Impedances

Transfer impedances were observed in order to determine the validity of the assumption of a linear structure. A more detailed discussion of the reasons for this phase of the investigation may be found in Section 2.5 which also describes the experimental arrangement employed.

The transfer impedances obtained experimentally are shown graphically in Fig. 14. The good correlation between these two curves indicates the validity of the reciprocity relation (equation (18)) and the assumption of linearity.

The Z vs f curves in Fig. 14 were plotted from M vs f curves. The values of effective mass used in plotting the original curves were the observed values. This means that the combined structure, consisting of cantilever beam, elastic mount, and impedance head, can be assumed to be linear.

There are a number of explanations for the displacement

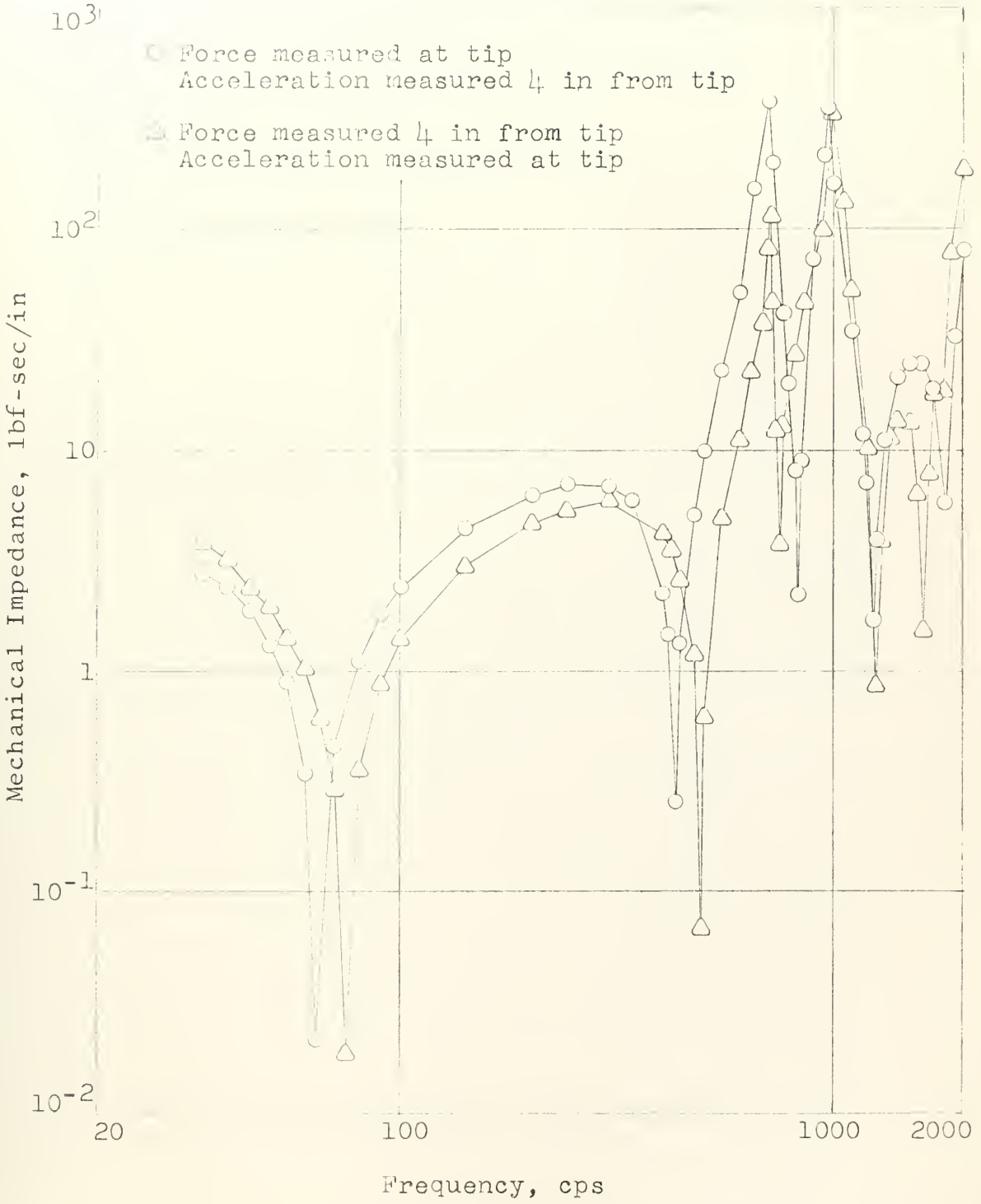

Fig. 14. Transfer Impedance (Uncorrected) as a Function of Frequency. Steel Cantilever Beam, 13 in x 2 in x 0.5 in. Elastic Hinge Drive. Verification of Reciprocity Relation.

of one of these curves with respect to the other.

(a) The manner of driving the beam was not the same for the two curves. Fig. 7 illustrates the arrangement for driving at the end of the beam. When driving the beam at a point four inches from the end, the elastic hinge was attached to the beam by means of a T-shaped connector.

(b) In obtaining both curves, it is likely that small errors in aligning and attaching the drive assembly to the beam resulted in the beam not being driven on its center line or perpendicular to this center line.

(c) Due to the manner in which the accelerometer was mounted, the distance between the points where force and acceleration were measured was 4.00 in for one curve and about 4.10 in for the other curve.

Considering these differences, the correlation between the two curves is considered very good.

4. Conclusions

1. The measurement of phase angles and transfer impedances confirmed qualitatively the validity of the assumptions of negligible damping and linearity which were made in the derivation of the receptance function for the cantilever beam.

2. The clamping jig when loaded by the universal testing machine was an effective means of achieving experimentally the 'clamped' end condition required for the cantilever beam.

3. The method of exciting the cantilever beam experimentally only approximated the sinusoidal excitation assumed in the theoretical development of the problem and its solution.

4. The accuracy with which phase angle information could be determined was the controlling factor in the accuracy of the results obtained. The error in phase angle determinations appears to vary with the magnitude of the phase angle. Estimates of the magnitudes of these errors may be found in Section 3.3.

5. The procedure used for determining phase angles, while marginally satisfactory for a small number of phase angles, is considered unsatisfactory for determining a

structures vibrated in this thesis, the nature of the structure and its response appear to be affected considerably by attaching the means of driving the structure and measuring the driving force and resultant motion. The effect of this attachment is that the effective mass measured by the impedance head is not the effective mass of the structure being studied. It is the effective mass of the system consisting of this structure, the accelerometer end of the impedance head, and the elements of the driving arrangement between them. This attachment appears to have introduced additional resonances and antiresonances in the experimentally-determined impedance functions.

7. As a result of this investigation, the use of theoretical impedance functions does not appear to be a reliable method of determining the resonant frequencies of structures such as machinery foundations. The difficulty experienced in realizing a true cantilever beam under laboratory conditions indicates the likelihood of a correspondingly greater difficulty in describing theoretically the structural elements in a foundation. Indications are that these members cannot be described by such simplified models. Due to the method of joining structural elements it seems reasonable to anticipate

that the theoretical end conditions will not be realized in an actual structure. It should be emphasized, however, that this observation is an extrapolation of the results of this investigation. The evidence is not conclusive. Continued investigation of this possibility appears to be desirable.

8. The difficulty of 'divorcing' the cantilever beam used in this investigation from the driving-measuring structure indicates the possibility of encountering similar problems in other impedance measurements, and in the interpretation of the results thereof.

9. The elastic hinge drive was effective in reducing lateral vibrations of the vibration generator at low frequencies. However, the 'spring-like' behavior of the elastic hinge itself introduced the additional problem of correcting the observed data to account for this behavior.

10. Good correlation between the theoretically-derived impedance function and that determined experimentally was obtained only in the vicinity of the first resonance and the first antiresonance of the cantilever beam. At other frequencies, correlation was adversely affected by (a) the accuracies of the phase angle determinations and signal voltage measurements, and (b) the resonances introduced by attaching the driving-measuring structure.

11. It was not always possible to reproduce data taken at an earlier time. This may be explained in part by (a) failure to achieve thermal equilibrium in the electronic instruments, and (b) minor differences in the alignment of the driving, measuring and driven structures.

12. Vibration of a pure mass provides an excellent method for checking theoretical relationships, experimental procedures, and the proper functioning of the measuring instruments.

13. The Endevco Model 2110 impedance head appears to be better suited to the measurement of the effective mass of structures larger (more massive) than those used in this investigation.

4. Recommendations

The following recommendations stem from experience gained in this thesis investigation:

1. That a suitable portion of each introductory course in mechanical vibrations be devoted to instruction in mechanical impedance methods. Coverage should include fundamental concepts, four pole parameter methods and at least one laboratory exercise to gain familiarity with impedance measuring instruments and techniques.

2. That graduate students be encouraged to pursue research, both theoretical and experimental, directed toward the solution of steady state vibration problems using mechanical impedance methods.

3. That more precise methods of determining phase angles be investigated.

4. That practical methods of obtaining continuous and direct readout of both impedance magnitude and phase angle information be investigated.

5. That additional research be directed toward the use of theoretical impedance functions as an adjunct to the design of foundation-like structures.

BIBLIOGRAPHY

1. American Standard Acoustical Terminology (Including Mechanical Shock and Vibration), S1.1-1960, New York, American Standards Association, 1960

2. Belsheim, R. O., Introductory Remarks, In "30th Symposium on Shock, Vibration and Associated Environments, Mechanical Impedance Session, Detroit, Oct. 10, 1961, (Preprints)." It is anticipated that the papers presented at this symposium will be published by the Office of the Secretary of Defense (Research and Engineering) as Shock, Vibration and Associated Environments, Bulletin No. 30.

3. Colloquium on Mechanical Impedance Methods for Mechanical Vibrations, New York, Dec. 2, 1958, New York, American Society of Mechanical Engineers, 1958

4. Hixson, Elmer L., Mechanical Impedance and Mobility, In Harris, Cyril M., and Charles E. Crede, eds., "Shock and Vibration Handbook," v. 1, New York, McGraw-Hill, 1961

5. Belsheim, R. O., and J. W. Young, Jr., Mechanical Impedance as a Tool for Shock or Vibration Analysis, NRL Report 5409, Washington, D.C., U. S. Naval Research Laboratory, Feb. 15, 1960

6. Simplified Vibration Analysis by Mobility and Impedance Methods, Cleveland 13, Ohio, The Penton Publishing Co., 1959, 1960. Articles by Richard F. Thorn and Austin H. Church reprinted from "Machine Design," v. 31, nos. 25 and 26, 1959; and v. 32, nos. 4, 5, 6, 7, 8, 9 and 11, 1960

7. Kinsler, Lawrence E., and Austin R. Frey, Fundamentals of Acoustics, New York, Wiley, 1950, p. 19-22

8. Hansen, H. M., and Paul F. Chenea, Mechanics of Vibration, New York, Wiley, 1952, p. 138-218

9. Freberg, C. R., and E. N. Kemler, Elements of Mechanical Vibration, 2nd ed., New York, Wiley, 1949, p. 174-197

10. MacDuff, John N., and John R. Curreri, Vibration Control, New York, McGraw-Hill, 1958, p. 40-50

BIBLIOGRAPHY

11. Young, J. W., Jr., and R. O. Belsheim, Experimental Measurement of Mechanical Impedance, NRL Report 5455, Washington, D.C., U. S. Naval Research Laboratory, May 24, 1960

12. Duncan, W. J., The Admittance Method for Obtaining the Natural Frequencies of Systems, Philosophical Magazine and Journal of Science (London), v. 32, no. 214, Nov., 1941, p. 401-409

13. Johnson, D. C., The Application of Admittance Methods in the Classical Theory of Small Oscillations, Engineering (London), v. 171, no. 4453, June 1, 1951, p. 650-652

14. Bishop, R. E. D., The Analysis of Vibrating Systems which Embody Beams in Flexure, The Institution of Mechanical Engineers, Proceedings (London), v. 169, 1955, p. 1031-1050

15. Bishop, R. E. D., and D. C. Johnson, The Mechanics of Vibration, Cambridge, England, Cambridge University Press, 1960

16. Bouche, R. R., Endevco Corporation, Pasadena, California, personal communication, Feb. 23,1962

17. Blake, Ralph E., Lockheed Missles and Space Co., Sunnyvale, California, personal communication, Nov. 20, 1961

18. Kolloy, J. T., Four Pole Parameters in Vibration Analysis, In "Colloquium on Mechanical Impedance Methods for Mechanical Vibrations," New York, American Society of Mechanical Engineers, 1958, p. 43-68

19. Endevco Corporation, Instruction Manual Model 2110 Impedance Head, Pasadena, California, 1961

20. Redfern, J. T., An Electrical Phase Shifter and Meter, Report 591, San Diego, California, U. S. Navy Electronics Laboratory, 9 March 1955

21. Coleman, G. M., Impedance and Power Transmission Detection on Mechanically Vibrated Structures, Report 602, San Diego, California, U. S. Navy Electronics Laboratory, 15 June 1955, (Confidential)

22. Den Hartog, J. P., Mechanical Vibrations, 4th ed., New York, McGraw-Hill, 1956

23. Timoshenko, S., and D. H. Young, Vibration Problems in Engineering, 3rd ed., Princeton, New Jersey, Van Nostrand, 1955

24. Van Santen, G. W., Introduction to a Study of Mechanical Vibrations, Eindhoven, Holland, Philips' Technical Library, 1953

25. Wright, D. V., and A. C. Hagg, Practical Calculation and Control of Vibration Transmission through Resilient Mounts and Basic Foundation Structures, Westinghouse Research Laboratories Report 405 FD 208-R2, Dec. 1, 1959. Bureau of Ships Contract NOBS 72326, Index No. NS-713-212

26. MacKinnon III, Malcolm, and James M. Taylor, An Analytic Study of Vibration Transmission in Typical Shipboard Installations, Masters Thesis, Massachusetts Institute of Technology, 1961

27. Bradley, Jr., Wilson, Mechanical Impedance Testing, Pasadena, California, Endevco Corporation

28. Plunkett, Robert, Experimental Measurement of Mechanical Impedance or Mobility, Journal of Applied Mechanics, American Society of Mechanical Engineers, v. 21, no. 3, Sep., 1954, p. 250-256

29. Plunkett, Robert, Semigraphical Method for Plotting Vibration Response Curves, In "Proceedings of Second U. S. National Congress of Applied Mechanics," New York, American Society of Mechanical Engineers, 1955

APPENDIX A

LIST OF EQUIPMENT AND INSTRUMENTS

RIEHLE Power Testing Machine Type PSC-120

Excitation Channel

DONNER Sine Wave Generator Model 1202

KRON-HITE Ultra-Low Distortion Power Amplifier Model UF-101

GOODMANS Vibration Generator Model 390A

HEWLETT-PACKARD Industrial Electronic Counter, Model 521A/C

Force and Acceleration Channels

ENDEVCO Impedance Head Model 2110

ENDEVCO Accelerometer Model 2215

ENDEVCO Cathode Follower (Drawing No. XC1066)

KRON-HITE Ultra-Low Frequency Band-Pass Filter Model 330-M

TEKTRONIX Oscilloscope Type 545 with High Gain Differential Calibrated DC Preamp (Type 53/54D Plug-In Unit)

HEWLETT-PACKARD Vacuum Tube Voltmeter Model 400D

Phase Angle Determination

HEWLETT-PACKARD Oscilloscope Model 130A

GENERAL RADIO Decade Resistor Type No. 1432-M

GENERAL RADIO Decade Condenser Type No. 219-M

APPENDIX B

FORTRAN PROGRAM FOR COMPUTING EFFECTIVE MASS AS A FUNCTION OF FREQUENCY FOR A TIP-DRIVEN CANTILEVER BEAM OF UNIFORM CROSS-SECTION (CONTROL DATA CORPORATION COMPUTER 1604)

```
      PROGRAM HOOVER
400   FORMAT (7F8.0)
      READ 400, B, H, ZL, RHO, E, X, GC
      A = B*H
      ZI = B*(H**3)/12.0
      I = 1
      DIMENSION FR(3000),AM(3000)
      DO 911 J = 1,3000
      FR = J
      R = 39.478*FR*FR*A*RHO/(E*ZI*GC)
      P = R**0.25
      F4 = COSF(P*ZL)*COSH(P*ZL)+1.0
      F7 = SINF(P*ZL)+SINH(P*ZL)
      F9 = COSF(P*ZL)+COSH(P*ZL)
      G1 = COSF(P*X)-COSH(P*X)
      G2 = SINF(P*X)-SINH(P*X)
      AM = -E*ZI*P**3*F4/(19.739*FR*FR*(F7*G1-F9*G2))
      FR(I) = FR
      AM(I) = AM
911   I = I+1
300   FORMAT(//10X,3(5X2HFR14X2HAM10X)//)
```

```
      PRINT 470
52 FORMAT (3(E10.5, G10.4))
      PRINT 52,(FR(I),AM(I),FR(1000+I),AM(1000+I),
     1FR(2000+I),AM(2000+I),  I = 1,1000)

      END
      END
```

APPENDIX C

DERIVATION OF EQUATIONS FOR DETERMINING PHASE ANGLES

Fig. 1-C is the circuit diagram of the lag network used in determining the phase angle by which one signal voltage was retarded in order to bring it into phase coincidence (or phase opposition) with a second signal voltage.

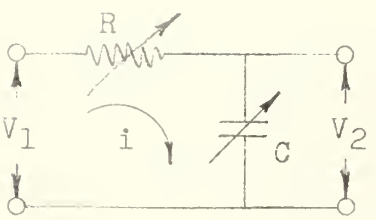

Fig. 1-C. Lag Network for Determining Phase Angles

Using loop current methods

$$i = \frac{V_1}{R - jX_C} \qquad (1\text{-}C)$$

$$V_2 = i(-jX_C) = \frac{V_1}{R - jX_C} \cdot (-jX_C) = V_1 \cdot \frac{1}{\frac{R}{-jX_C} + 1} = V_1 \cdot \frac{1}{j\omega RC + 1} \qquad (2\text{-}C)$$

It follows from equation (2-C) that V_2 lags V_1 by the angle

$$\alpha = \arctan \omega RC \qquad (3\text{-}C)$$

In Section 1.3, θ is defined as the angle by which

force leads acceleration.

If the two signal voltages mentioned above are V_F and V_a, and if the two signals are brought into phase by the lag network, (indicated by a positive slope of the major axis of the ellipse on the oscilloscope,)

$$\theta = 180^\circ \text{ (due to polarity of impedance head signals)} + \alpha \tag{4-C}$$

if V_F is retarded. See Fig. 2-C.

$$\theta = 180^\circ \text{ (due to polarity of impedance head signals)} - \alpha \tag{5-C}$$

if V_a is retarded. See Fig. 3-C.

If the two signals are brought into phase opposition by the lag network, (indicated by a negative slope of the major axis of the ellipse on the oscilloscope,)

$$\theta = 0^\circ \text{ (due to polarity of impedance head signals)} + \alpha \tag{6-C}$$

if V_F is retarded. See Fig. 4-C.

$$\theta = 0^\circ \text{ (due to polarity of impedance head signals)} - \alpha \tag{7-C}$$

if V_a is retarded. See Fig. 5-C.

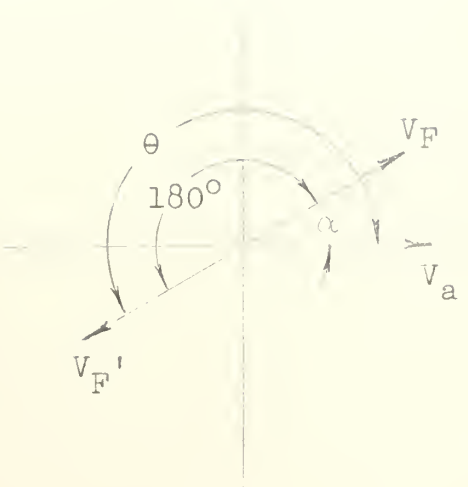

Fig. 2-C. Phase Angle Determination. Positive Slope. V_F Retarded.

$\theta = 180^\circ + \alpha$

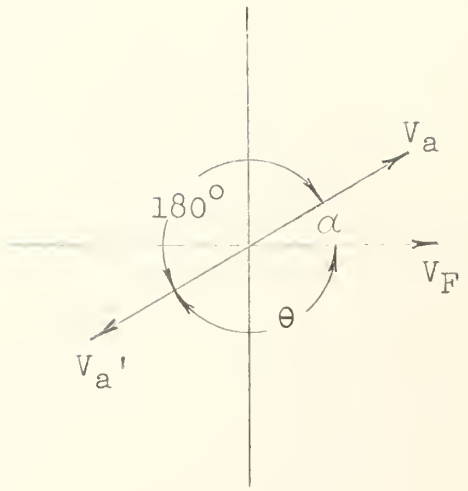

Fig. 3-C. Phase Angle Determination. Positive Slope. V_a Retarded.

$\theta = 180^\circ - \alpha$

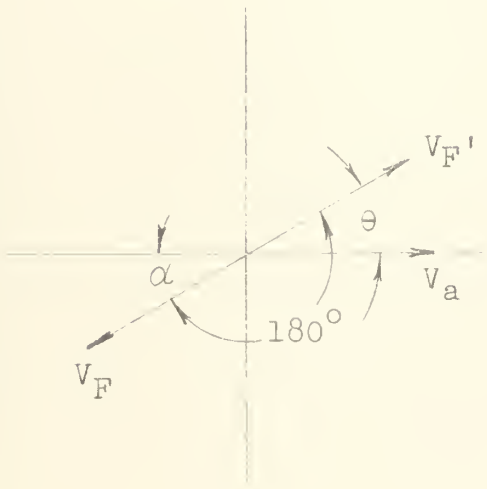

Fig. 4-C. Phase Angle Determination. Negative Slope. V_F Retarded.

$\theta = \alpha$

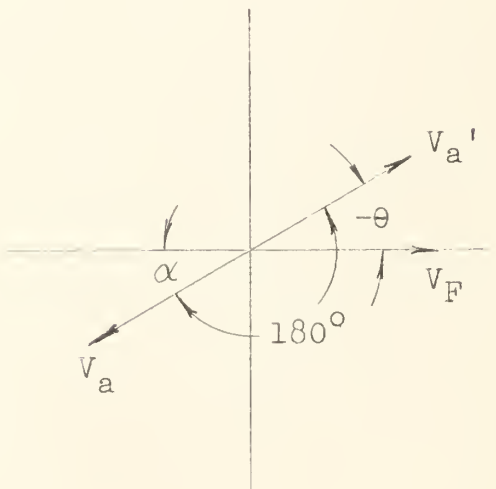

Fig. 5-C. Phase Angle Determination. Negative Slope. V_a Retarded.

$\theta = -\alpha$

APPENDIX J

It is necessary to add (or subtract) 180° to phase angles determined by comparing V_F and V_a as they come from the impedance head. The explanation for this lies in the manner in which the piezoelectric crystal transducer elements are mounted in the impedance head. [19]

APPENDIX D

SAMPLE CALCULATIONS

The calculations contained in this appendix are provided to illustrate the method of determining experimentally the effective mass of the cantilever beam described in Section 2.2. The calculations given below are those required to determine one point on the M vs f curve from which Fig. 11 was plotted, and one point on the ϕ vs f curve (Fig. 12), for the direct drive configuration illustrated in Fig. 4.

The symbols used in these calculations which were not included in the Table of Symbols are defined as follows:

Subscripts

a acceleration channel

b beam

c correction

F force channel

o observed

s supplied by manufacturer

t transducer

x external

APPENDIX D

The following data were taken at the data point selected for these calculations. Sensitivities and other characteristics of the instrumentation which are required for the calculations are also included.

$G_a = 0.857$ $\quad C_{ta} = 1676$ pf

$G_F = 0.850$ $\quad C_{tF} = 997$ pf

$E_{sa} = 51.5$ rms mv/peak g $\quad C_{xa} = 107$ pf

$E_{sF} = 5.00$ rms mv/peak lbf $\quad C_{xF} = 109$ pf

$f = 379$ cps $\quad R = 1000$ ohms

$V_F = 13.7$ mv rms $\quad C = 2.6 \times 10^{-7}$ farad

$V_a = 66.0$ mv rms $\quad$ slope of ellipse: negative

V_a retarded

The 'GE ratio' given in equation (1-D) was defined to facilitate the calculations. This ratio remains the same for any given drive arrangement and combination of instruments. [19]

$$\text{GE ratio} = \frac{(GE)_a}{(GE)_F} = \frac{G_a}{G_F} \cdot \frac{E_{sa}(C_{ta} + 100)}{(C_{ta} + C_{xa})} \cdot \frac{(C_{tF} + C_{xF})}{E_{sF}(C_{tF} + 100)} \qquad (1\text{-}D)$$

$$= \frac{0.857}{0.850} \cdot \frac{51.5 \text{ rms mv}}{\text{peak g}} \cdot \frac{(1676 + 100)\text{pf}}{(1676 + 107)\text{pf}} \cdot \frac{\text{peak lbf}}{5.00 \text{ rms mv}}$$

$$\cdot \frac{(997 + 109)\text{ pf}}{(997 + 100)\text{ pf}}$$

$$\text{GE ratio} = 10.33 \frac{\text{peak lbf}}{\text{peak g}}$$

APPENDIX D

The observed effective mass M_o is determined using equation (11) in Section 1.3.

$$M_o = \frac{F_o}{a_o} = \frac{V_F}{V_a} \cdot \text{GE ratio} \qquad (2\text{-D})$$

$$M_o = \frac{13.7 \text{ mv rms}}{66.0 \text{ mv rms}} \cdot \frac{10.33 \text{ peak lbf}}{\text{peak g}} = \frac{2.15 \text{ peak lbf}}{\text{peak g}}$$

$$M_o = 2.15 \text{ lbm}$$

The phase angle θ_o associated with M_o is determined by ω, R, C, the slope of the ellipse, and the signal voltage which is retarded. These relations are developed in Appendix C.

$$\alpha = \arctan \omega RC \qquad (3\text{-C})$$

$$\alpha = \arctan (2\pi)(379 \text{ cps})(1000 \text{ ohms})(2.6 \times 10^{-7} \text{ farad})$$

$$= \arctan 0.618$$

$$\alpha = 31^\circ 44'$$

$$\theta_o = 0^\circ - \alpha = -31^\circ 44' \qquad (7\text{-C})$$

The effective mass of the beam M_b and the phase angle associated with it θ_b, are determined from the following equation: [19]

$$M_b e^{j\theta_b} = M_o e^{j\theta_o} - M_c e^{j\theta_c} \qquad (3\text{-D})$$

APPENDIX A

of the structure between the impedance head and the beam acts as a pure mass, the value of M_c in equation (3-5) is the sum of the effective mass of the accelerometer end of the impedance head, the mass of the adapter, and the mass of that part of the steel stud between the center plane of the impedance head and the beam. [16] It was verified experimentally that this 'package' did, in fact, act as a pure mass. At 379 cps, $M_c = 0.743$ lbm and $\theta_c = 0°$.

Equation (3-5) can also be written

$$M_b e^{j\theta_b} = M_c \cos\theta_o + jM_o \sin\theta_o - M_c \cos\theta_c - jM_c \sin\theta_c \qquad (4-5)$$

$$M_b e^{j\theta_b} = 2.15 \text{ lbm} \cos(-31°44') + j2.15 \text{ lbm} \sin(-31°44') - 0.743 \text{ lbm} \cos 0°$$

$$= 1.83 \text{ lbm} - j\,1.132 \text{ lbm} - 0.743 \text{ lbm}$$

$$= 1.09 \text{ lbm} - j\,1.132 \text{ lbm}$$

$$= 1.57 \text{ lbm}\, e^{j(-46°08')}$$

$M_b = 1.51$ lbm and $\theta_o = -46°08'$ are plotted at f = 379 cps in Figs. 11 and 12 respectively.

In order to check the value of θ_o determined above, a second determination was made using the alternate ('indirect') procedure described in Section 2.6. The data

and calculations for this second determination are summarized in Table 1-D and in Fig. 1-D.

Signal Retarded	Slope of Ellipse	R (ohms)	C (farads)	ωRC	α
V_F	negative	1000	6×10^{-9}	0.0243	0°49'
V_a	positive	1000	3.42×10^{-7}	.815	39°12'

Table 1-D. Data and Calculations for Determining θ_o by the Alternate Procedure Described in Section 2.6. f = 379 cps.

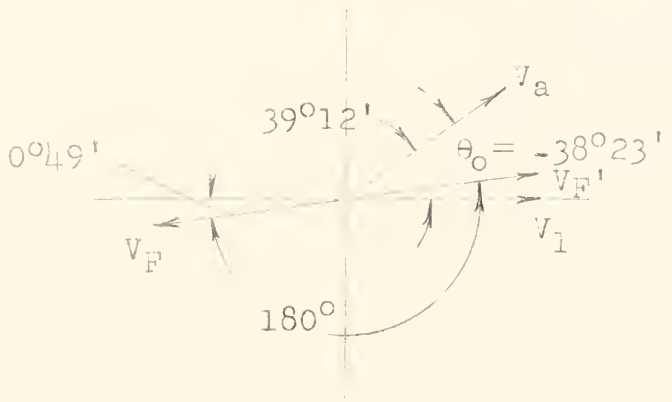

Fig. 1-D. Determination of θ_o at f = 379 cps by Comparing V_F and V_a with a Reference Voltage V_1. θ_o = -38°23'.

At this frequency, and with the above data, there was no reason to think that one of the phase angles so determined was more accurate than the other. The difference of 6°39' is indicative of the accuracy to which phase angles

of this magnitude can be determined using the procedures which were used in this investigation. This points up the need for a more precise method of phase angle determination. For a more detailed discussion of the errors involved in phase angle observations, see Section 3.3.